Science of the Total Environment xxx (2013) xxx–xxx

Contents lists available at ScienceDirect

Science of the Total Environment

journal homepage: www.elsevier.com/locate/scitotenv

Differentiating transpiration from evaporation in seasonal agricultural wetlands and the link to advective fluxes in the root zone

P.A.M. Bachand [a,*], S. Bachand [a], J. Fleck [b], F. Anderson [b], L. Windham-Myers [c]

[a] Tetra Tech, Davis, CA, United States
[b] U.S. Geological Survey, California Water Science Center, Sacramento, CA, United States
[c] U.S. Geological Survey, National Research Program, Menlo Park, CA, United States

HIGHLIGHTS

- PFR model utilizes EC as conservative tracer to calculate transpiration rates.
- Wetland transpiration causes significant summertime percolation into the root zone.
- A Peclet number equivalent relationship is derived for evaluating root zone fluxes.
- Transpiration affects soil diffusive and advective flux vertical distribution.
- Transpiration causes seasonal/diel trends in benthic fluxes of Hg and other constituents.

GRAPHICAL ABSTRACT

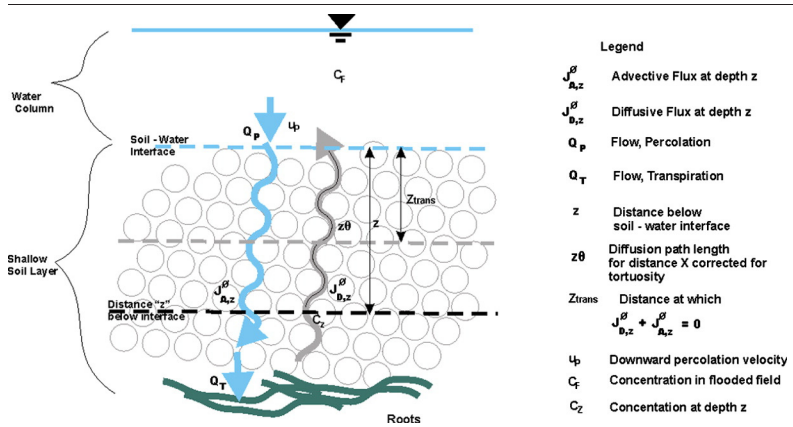

ARTICLE INFO

Article history:
Received 5 August 2012
Received in revised form 5 November 2013
Accepted 5 November 2013
Available online xxxx

Keywords:
CFSTR
PFR
Peclet number
Tracers
Methylmercury
Benthic flux

ABSTRACT

The current state of science and engineering related to analyzing wetlands overlooks the importance of transpiration and risks data misinterpretation. In response, we developed hydrologic and mass budgets for agricultural wetlands using electrical conductivity (EC) as a natural conservative tracer. We developed simple differential equations that quantify evaporation and transpiration rates using flow rates and tracer concentrations at wetland inflows and outflows. We used two ideal reactor model solutions, a continuous flow stirred tank reactor (CFSTR) and a plug flow reactor (PFR), to bracket real non-ideal systems. From those models, estimated transpiration ranged from 55% (CFSTR) to 74% (PFR) of total evapotranspiration (ET) rates, consistent with published values using standard methods and direct measurements. The PFR model more appropriately represents these non-ideal agricultural wetlands in which check ponds are in series. Using a flux model, we also developed an equation delineating the root zone depth at which diffusive dominated fluxes transition to advective dominated fluxes. This relationship is similar to the Peclet number that identifies the dominance of advective or diffusive fluxes in surface and groundwater transport. Using diffusion coefficients for inorganic mercury (Hg) and methylmercury (MeHg) we calculated that during high ET periods typical of summer, advective fluxes dominate root zone transport except in the top millimeters below the sediment–water interface. The transition depth has diel and seasonal trends, tracking those of ET. Neglecting this pathway has profound implications: misallocating loads along different hydrologic pathways; misinterpreting seasonal and diel water quality trends; confounding Fick's First Law calculations when determining diffusion fluxes using pore water concentration data; and misinterpreting biogeochemical mechanisms affecting dissolved constituent cycling in the root zone. In addition,

* Corresponding author at: Tetra Tech, Research & Development, 509 4th Street, Suite D, Davis, CA 95616, United States. Tel.: +1 530 564 4591.
E-mail address: Philip.Bachand@Tetratech.com (P.A.M. Bachand).

0048-9697/$ – see front matter © 2013 Elsevier B.V. All rights reserved.
http://dx.doi.org/10.1016/j.scitotenv.2013.11.026

Please cite this article as: Bachand PAM, et al, Differentiating transpiration from evaporation in seasonal agricultural wetlands and the link to advective fluxes in the root zone, Sci Total Environ (2013), http://dx.doi.org/10.1016/j.scitotenv.2013.11.026

our understanding of internal root zone cycling of Hg and other dissolved constituents, benthic fluxes, and biological irrigation may be greatly affected.

© 2013 Elsevier B.V. All rights reserved.

1. Introduction

In wetlands, transpiration accounts for between 50 and 90% of the total ET during a growing season (Herbst and Kappen, 1999; Sanchez-Carrillo et al., 2004; Bouman et al., 2005). It is an important vector for moving constituents from the water column into the root zone in shallow aquatic systems (Howes et al., 1986; Hayashi et al., 1998; Reddy et al., 1999; Kadlec, 1999; Whitmer et al., 2000; Parsons et al., 2004; van der Kamp and Hayashi, 2009). Dacey and Howes (1984) determined transpiration as the primary cause for downward movement of the water table during both day and night in the short grass zone in intertidal salt marshes. Rosenberry et al. (2013) report that seepage in a Minnesota lake changed 10% during the day in response to ET withdrawals. Using a Br tracer study in a seasonal wetland, Parsons et al. (2004) found that less than 10% of the Br initially released was taken up by plants and most of the Br was transported into the upper 40–80 cm of the wetland soil surface. They describe how ET drives infiltration rates in seasonal wetlands, with infiltration rates increasing during summer periods of high evaporation. In a review paper on prairie wetlands of northern USA and Canada, van der Kamp and Hayashi (2009) describe how infiltration in the upper few meters of those wetlands is driven by evaporation and root uptake. A number of constituent cycling studies using bromide (Br) tracers have shown applied Br concentrating in the soil root zone and plant tissues (Howes et al., 1986; Whitmer et al., 2000; Parsons et al., 2004).

Transpiration has also been linked to transport and release of mercury (Hg) and volatile organic compounds from wetlands. Lindberg et al. (2002) determined that the flux of elemental Hg vapor (Hg^0) from rooted emergent cattail and sawgrass wetlands in the Florida Everglades significantly exceeded emissions from non-vegetated areas and from uprooted (floating) stands. A strong correlation with water vapor suggested transpiration as the driving mechanism. Mercury vapor fluxes exhibited a diel cycle with two peaks, and Lindberg et al. (2002) proposed two different gas exchange dynamics: early morning lacunal gas releases and midday transpiration releases. Lindberg et al. (2005) concluded that Hg^0 emitted from emergent macrophytes originates as inorganic Hg^{2+} in the sediments where it is reduced to Hg^0; they confirmed the two processes earlier proposed by Lindberg et al. (2002). Their mass balance calculations estimated that a release of Hg^0 is 1 kg yr^{-1} from a 1500 ha wetland, 20 times the amount evaded from the water surface. Reid and Jaffé (2012) found a similar result with emissions of volatile organic compounds from wetlands to be linked with transpiration.

Despite its physical role in vegetated systems, transpiration is not often included in the wetland biogeochemistry literature in consideration of benthic fluxes. Root hairs provide a large surface area that moves water from soil to plants (Raven et al., 1999). During periods of rapid transpiration, soils adjacent to the root zone may lack sufficient water, resulting in a hydraulic pressure gradient moving water towards root hairs (Taiz and Zeiger, 1991; Raven et al., 1999). This bulk movement of water is an advective process. Yet, benthic flux, defined as the transport of dissolved constituents between the water column and the underlying sediments, has included as transport mechanisms bioturbation, advection from biological irrigation, and diffusion (Kuwabara et al., 1999). Bioturbation is important in wetland systems (Fanjul et al., 2011; Kuwabara et al., 2012), affecting both the direction and magnitude of benthic flux between the water column and sediments by its effect on benthic metabolism and nutrient cycling (Fanjul et al., 2011). While some arid wetland research has implied the phenomenon of "biologic tides" from daily transpiration (e.g. Childers et al., Arizona State University, unpublished data), advective flux has largely been linked to natural biological irrigation in which benthic organism activities enhance the exchange of interstitial pore water over pure diffusion (Choe et al., 2004; Hammond et al., 1985). Reddy et al. (1999) and Kadlec (1999) do discuss transpiration's role in moving nutrients into the root zone through bulk water movement. In wetland systems, diffusive flux of Hg from the sediment column to the water has been primarily assessed by chamber flux measurements and modeled by concentration gradients (Gill et al., 1999; Holmes and Lean, 2006; Rothenberg et al., 2008), similar to many other dissolved constituents (Krottje, 1980; Reddy et al., 1980, 1984; Dunne et al., 2010). Both diffusive fluxes and biological irrigation have been measured to determine benthic fluxes of methylmercury (MeHg) and total mercury (THg) from San Francisco Bay Delta sediments into the water column in tributary streams, waterways and open water (Choe et al., 2004).

The wetland biogeochemistry literature also does not adequately consider transpiration and its role with regard to advective transport from the water column to the sediments in the development of water and mass balances. Though methods exist to directly or indirectly determine evaporation and transpiration separately in agricultural wetlands (Bethune et al., 2001; Bouman et al., 2005, 2007), most wetland studies, and water or mass balance analyses aggregate these two terms into ET (Mitsch and Gosselink, 1993; Kadlec and Knight, 1996; Kadlec, 2000; Bethune et al., 2001; Carleton et al., 2001; Martinez and Wise, 2003; Playan et al., 2008) despite these being very different hydrologic and transport processes. Whether implicit or explicit, this assumption is dominant in foundational literature (Mitsch and Gosselink, 1993; Kadlec and Knight, 1996) as well as in the development of reactor models (Metcalf and Eddy, 2009; Kadlec, 1994, 2000; Werner and Kadlec, 2001; Martinez and Wise, 2003; Persson and Wittgren, 2003; Carleton and Montas, 2009), and quantification of benthic flux (Romkens and Bruce, 1964; Krottje, 1980; Reddy et al., 1980, 1984; Gill et al., 1999; Langer et al., 2001; Holmes and Lean, 2006).

Not differentiating evaporation and transpiration flow paths may generate large errors in quantifying Hg budgets and within-agricultural wetland cycling and storage processes. As part of a multi-disciplinary process-based study of Hg cycling on wetlands of California's Central Valley, we assessed hydrologic flows on six agricultural wetlands and two naturally vegetated managed wetlands over a full annual cycle. Our initial analyses did not differentiate between evaporation and transpiration. The resulting hydrologic budget was inconsistent with chloride and isotope mass budgets, thus affected our analyses of Hg cycling in the systems. Our inability to reconcile the calculations made us reassess the approach, especially concerning downward advection by root-driven transpiration and its effect on subsurface transport and cycling.

We hypothesized 1) that transpiration-driven advection provides a significant transport pathway to the root zone during the summer months, and 2) that this process leads to seasonal and diel changes in concentrations of conservative tracers, thus potentially affecting concentrations and speciation of Hg as well. To address the first hypothesis and quantify transpiration and evaporation pathways, we integrated a hydrologic balance with an electrical conductivity (EC) mass balance. We used wetland hydrologic and water quality data from the crop year May 2007–May 2008 in these models. Electrical conductivity (EC) was used as a natural conservative tracer, similar to what has been done with salts in other systems (Hayashi et al., 1998; Whitmer et al., 2000; Parsons et al., 2004; Pellerin et al., 2007). We applied two different mass balance models to assess water dynamics in the eight study wetlands. These two ideal models represented two extremes for surface water mixing: (1) a plug flow reactor (PFR) model that assumes no mixing along the flow gradient and (2) a continuous flow stirred tank reactor (CFSTR) model that assumes

Please cite this article as: Bachand PAM, et al, Differentiating transpiration from evaporation in seasonal agricultural wetlands and the link to advective fluxes in the root zone, Sci Total Environ (2013), http://dx.doi.org/10.1016/j.scitotenv.2013.11.026

complete mixing. This approach, the integration of the EC mass balance with a hydrologic balance, would enable us to calculate transpiration and evaporation rates in a novel way; and would provide a simple method for separating evaporation from transpiration in the analyses of wetland systems. This method also would require little additional water quality data that is typically collected in assessing these systems and provide important information on transport pathways. Natural tracers like chloride and EC are commonly measured and in the case of EC can be measured easily in situ with datasondes.

To address the second hypothesis, we quantified the magnitudes of diffusive and transpiration-driven advective fluxes (J_A) for dissolved constituents. These are downward fluxes from the water column into the root zone driven by plant transpiration. This analysis includes Hg, which is of particular interest for this multi-disciplinary process-based study on California Central Valley wetlands. These analyses provide insight into Hg exchanged between surface and subsurface waters (Bachand et al., in this issue) and movement in the root zone (Windham-Myers et al., in this issue-b), and quantify soil storage and transport pathways in wetland systems. From these analyses, we discuss the implications with regard to internal root zone cycling of Hg and other dissolved constituents, benthic flux interpretations, wetland water and mass budget calculations, and diel and seasonal sediment flux trends.

2. Materials and methods

In this section, we describe the study site; explain the experimental design justifying the hydrologic data and the methods used for data collection; present methods used for determining evaporation; present the derivation and integration of the water and mass balances for discriminating transpiration rates from evaporation rates; present the root zone flux model derivation for determining transition depths between advective and diffusive fluxes; provide a discussion of data analyses and QAQC; and discuss sources of uncertainty.

2.1. Site description

The Yolo Bypass (Yolo Bypass) is a historic floodplain of the Sacramento River watershed now managed as a 24,000 ha flood control spillway. Yolo Bypass is underlain by poorly drained silty clay loams of the Sacramento Series (Soilweb, 2011), structured as a textured alluvium of 60–70% clay in the upper meter, with 78% of sediment particles as silt and clay (<63 μm) in the upper 2 cm across all agricultural wetlands (Marvin-DiPasquale et al., in this issue). Within the Yolo Bypass is the Yolo Bypass Wildlife Area, which is home to numerous species and includes agricultural fields. Rotational rice agricultural wetlands (conventional rice, wild rice, and fallowed fields) were established in this area through the establishment of berms and appropriate water management. Historically sourced from the Sacramento River and multiple Sierra and Coast Range tributaries (Springborn et al., 2011), the Yolo Bypass Wildlife Area sediments are elevated in Hg due to the legacy of hydraulic gold mining in the Sierra Nevada and Hg mining in the Coast Ranges (Alpers et al., 2005). The Yolo Bypass Wildlife Area also encompasses a wide range of non-agricultural wetlands (Windham-Myers et al., in this issue-a). Non-agricultural wetlands managed for wildlife include permanently flooded wetlands and seasonal wetlands flooded consistently with annual river stage and precipitation events.

Our study focused on eight wetlands, ranging in size from 16 to 78 ha (Fig. SI 1). Agricultural wetlands included: replicated rice fields (*Oryza sativa*, n = 2, R31 and R64), replicated wild rice fields (*Zizania palustris*, n = 2, W32 and W65) and replicated fallowed fields (dominated by bare ground and agricultural weeds e.g., *Alisma* and *Cyperus* spp., n = 2, F20 and F66) (Fig. SI 1). The replicate agricultural wetlands were distributed evenly across the two blocks of distinct water sources — northern fields (R31, W32, and F20) and southern fields (R64, W65, F66; Windham-Myers et al., in this issue-a). This study assessed the hydrologic interactions related to evaporation and transpiration which depended upon agricultural management with regard to crop establishment, planting and harvest. While the fields generally served as good replicates for hydrologic fluxes (e.g. Fig. SI 2), they varied in initial water quality (Alpers et al., in this issue). Southern agricultural wetlands received tidally pumped Sacramento River water as an irrigation source; northern agricultural wetlands were a mix of tidally pumped river water and discharge water from agricultural wetlands recycled for irrigation (Fig. SI 1; Windham-Myers et al., in this issue-a,b,c). We also investigated non-agricultural wetlands: a 52 ha seasonally flooded wetland (seasonal wetland) dominated by swamp timothy (*Crypsis schoenoides*) flooded in fall and winter, and a 16 ha permanently flooded wetland (permanent wetland) dominated by open water with floating (*Ludwigia petiolata*) and emergent vegetation (*Typha* spp. and *Scheonoplectus acutus*) along the littoral zone.

Each agricultural wetland was managed in accordance with the agronomic needs of each crop (Table SI 1). The agricultural wetlands – rice (R31 and R64), wild rice (W32 and W 65), fallowed (F20 and F66) – were drained to enable preparation and early planting beginning March 1, 2007 (Fig. 1; Table SI 1). By May 1 and into June, rice and wild rice agricultural wetlands were sufficiently dry to remove weedy vegetation by tilling using a disk and leveling. In fall, water levels were dropped depending upon each crop need with levels in fallowed fields dropped earliest (Table SI 1). Rice fields were drained in September for dry rice harvest. As wild rice is wet harvested, inflows to these fields were stopped in fall but water levels were not dropped immediately. All fields were flooded again by late fall to decompose rice residues. Between January and February Yolo Bypass and Yolo Bypass Wildlife Area were managed for flood control of the Sacramento River, resulting in rapid water level rise in the agricultural wetlands, overtopping berms throughout. Table SI 1 summarizes management practices and Table SI 2 quantifies general hydrology (length and depth of inundation, irrigation volumes). Overall, replicated crop fields were managed similarly with regard to planting dates, inundation schedule, fertilization, harvest dates and winter flooding.

2.2. Hydrologic data

Each agricultural wetland was subdivided into a series of checks or ponds along elevation contours separated by berms (Fig. SI 3, Table SI 2). These checks are established to enable a rice field to be uniformly flooded despite a large elevation, or fall, across the field. Each check was established to enable a 5–8 cm of fall across each check in order to maintain relatively uniform water depths. Weirs were placed at checks and field outflows to manage water levels and flows (Fig. SI 3). Surface water from the agricultural wetlands was discharged into outflow ditches and drains.

We defined hydrologic units (HUs) within each agricultural wetland to measure hydrology based on the most upstream and downstream weir structure(s) (Table SI 3, Fig. SI 3). Staff gauges and pressure transducers were installed at HU inflow and outflow weirs to monitor flow rates. Water flow rates over a weir were estimated under critical flow conditions by measuring the head over the weirs and using the standard engineering equation (Heald, 2002):

$$Q = C(L - 0.2H)H^{1.5} \quad (1)$$

where Q = flow in cubic feet per second, L = length of weir opening in feet, H = head on weir in feet and C = weir coefficient A C-value of 3.207 ($r^2 = 0.94$) was used based on calibrated results on similar weir systems (Bachand and Associates et al., 2006). During the irrigation season, we collected hydrologic measurements every 3–4 days during midday (10 AM–2 PM). During the winter period, collection frequency decreased due to site access restrictions from flooding and hunting season scheduling requirements. Additional field measurements included: staff gauge water elevation; pH, EC, and temperature using a YSIs 6920 V2 sonde (YSI, Yellow Springs, Ohio); and surface water samples

ARTICLE IN PRESS

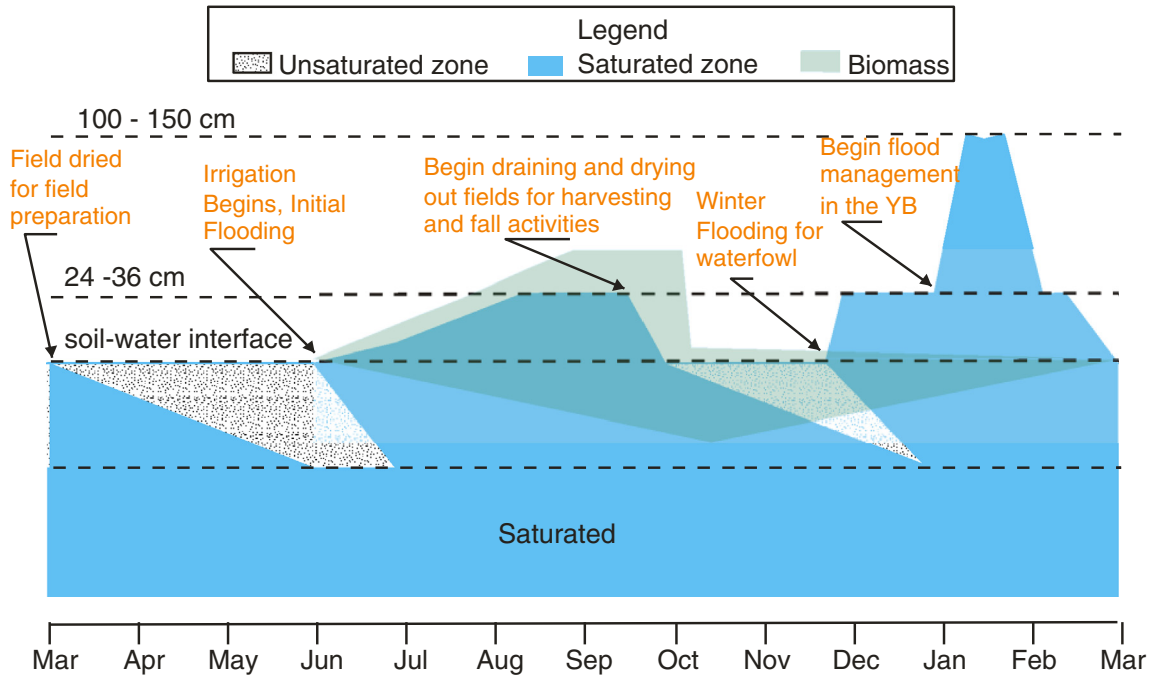

Fig. 1. Conceptual model of surface–subsurface hydrology in rice fields. Each crop has similar management though the timing and duration of each management event are different. Fields are dried out around March to allow for agricultural wetland preparation. Crops are planted around May and initial flooding begins. Crops accumulate above and below ground biomass and then are harvested around October for white rice, and September for wild rice. Above and below ground biomass disappears over the remaining fall and winter. Regional winter management leads to very high water levels. Flooding and drying out of unsaturated zones are modeled as top down. Both ground and surface waters are available to vegetation to meet evapotranspiration needs.

for analyses of chloride, MeHg, and other dissolved constituents relevant to the study. Methods regarding analysis of the dissolved constituents can be found in Alpers et al. (in this issue). Pressure transducer data was downloaded monthly to provide continuous water level data.

As agricultural wetland soils were unsaturated during initial flooding (Fig. 1), flow measurements could not be made for 2–4 weeks using the weir equation. We estimated inflow volume during initial flooding for wild rice agricultural wetlands as the combination of water needed to saturate the unsaturated soil above the plow sole and water level in the agricultural wetland at the end of the initial flooding phase (Fig. 1). Several studies have shown, through empirical data or modeling, that water does not quickly infiltrate past the plow sole in rice agricultural wetlands (Bouman et al., 1994; Wopereis et al., 1994; Liu et al., 2001). As the soils for our study have poor drainage and about an 18 cm deep plow layer (Soilweb, 2011), we estimated initial soil water content of 25% based upon agricultural wetland capacity of 30–35% and its hygroscopic coefficient (wilting point) of 10–18% (Soilweb, 2011; Brady and Weil, 2002). We estimated that 6 cm of water was needed to saturate the soil in the plot layer based on a porosity of about 50% for cultivated soils (Brady and Weil, 2002), which was in keeping with Marvin-DiPasquale et al. (60 ± 2%, this issue). By doubling this value to address any loss below the plow sole, we added 12 cm of water to the amount necessary to raise surface water levels, and flow rates were calculated based on the elapsed time during this period.

Fallowed agricultural wetland hydrologic management differed slightly from the rice agricultural wetlands. These fields were managed to minimize outflows, providing only enough water to meet ET demand. Thus, these fields typically had no outflows. Although initial irrigation was unregulated and could not be measured, management of these fields was similar across the entire irrigation season. We thus used this consistency to extrapolate initial flooding flow rates (when measurements were not taken) from average measured flows later in July.

2.3. Evapotranspiration

Reference ET (ET_o) and precipitation data were based on weather data from the California Department of Water Resources, California Irrigation Management Information System (CIMIS) (http://wwwcimis.water.ca.gov/cimis/welcome.jsp). Data was collected from CIMIS Station #6, in Davis, CA, approximately 15 km to the northwest of the agricultural wetlands. From water years 2000/2001–2009/2010 (July–June), ET_o was 143 ± 2 cm y^{-1} and precipitation was 42 ± 3 cm y^{-1}. Water year 2007/2008 had higher than average ET_o (154 cm y^{-1}) and average precipitation (42 cm y^{-1}). Crop coefficients were obtained from the California Department of Water Resources, Land Water Use Division (http://www.water.ca.gov/landwateruse/). Daily rates of ET_o were calculated using a program based on the standardized Penman Monteith equation (Penman, 1948). Actual ET was estimated for each crop by multiplying ET_o by the crop coefficient (K_c):

$$ET = K_c\, ET_o. \tag{2}$$

Values of K_c change temporally and differ between crop types (Fig. SI 4). During the growing season, K_c was based on crop development stage, as defined by the Food and Agriculture Organization Irrigation and Drainage Paper 56 (FAO 56) (Allen et al., 1998). Values for white rice were based on a local study of domestic rice (R. Snyder, personal communication), and actual ET values were in keeping with those measured by eddy-covariance in a nearby rice agricultural wetland (Hatala et al., 2012). Values for wild rice were taken as equal to those for wetlands with short vegetation (Allen et al., 1998). The permanent wetland is composed of 90% open water and a 10% perimeter of *Scheonoplectus/Typha* spp.; thus the K_c value for the open water was set according to pan evaporation and the K_c for the remaining 10% was set equal to values measured between 2002 and 2004 in a nearby study (Drexler et al., 2008). The K_c for the seasonal wetland was set

Please cite this article as: Bachand PAM, et al, Differentiating transpiration from evaporation in seasonal agricultural wetlands and the link to advective fluxes in the root zone, Sci Total Environ (2013), http://dx.doi.org/10.1016/j.scitotenv.2013.11.026

based on moist soil, as the site had no standing water during the growing season but sparse cover of ruderal species (e.g. *Crypsis shoenoides*). Values applied for the non-growing season were determined based on inundation, vegetation greenness, soil water content data, and from agricultural wetland notes and photographs provided by field staff.

2.4. Hydrologic and mass budgets

Hydrologic budgets and tracer mass budgets to calculate hydrologic fluxes into and out of the system along the various pathways (i.e. surface, subsurface, evaporation, transpiration) were derived. These derivations were the foundations of load calculations (Bachand et al., in this issue) and water quality analyses (Alpers et al., in this issue). These derivations also provided a means to parse out surface and subsurface flow paths from the total hydrologic and mass budgets, and to separate ET into its two components: evaporation and transpiration. The determination of transpiration then formed the foundation for a soil flux model that compared the magnitude of diffusive and transpiration-driven advective fluxes.

2.4.1. Identifying separate pathways for evaporation and transpiration

A mass budget was developed where surface and subsurface budgets were defined. Typical wetland mass balances integrate evaporation and transpiration into a single evapotranspiration term (ET; Fig. 2a) but these pathways differ because evaporation concentrates constituents in surface waters and transpiration transports dissolved constituents into the shallow root zone (Fig. 2b). The total water budget was described with the following expression:

$$Q_i + Q_{SSF} + Q_{Pr} = Q_o + Q_{ET} + \frac{dV}{dt} \quad (3)$$

where Q_i = surface flow into the system; Q_{SSF} = subsurface flow into the system; Q_{Pr} = flow into the system from precipitation; Q_o = surface flow out from the system; Q_{ET} = flow out from the system as evapotranspiration; and $\frac{dV}{dt}$ = change in water volume due to changes in surface water level, increasing as surface water levels increase. Surface flows onto and off of the system were normalized against agricultural wetland area (A_F) resulting in a hydraulic loading rate (HLR; cm d^{-1}) for inflows and outflows where:

$$HLR = Q/A_F. \quad (4)$$

Using the soil–water interface as a boundary between the surface and subsurface hydrologic balances, a surface water budget can be described by:

$$Q_i + Q_{Pr} = Q_o + Q_P + Q_E + \frac{dV}{dt} \quad (5)$$

where Q_P = flow out of system from percolation; and Q_E = flow off (out from) the water surface as evaporation. For flooded agricultural wetlands, soil in the root zone can be assumed to remain saturated

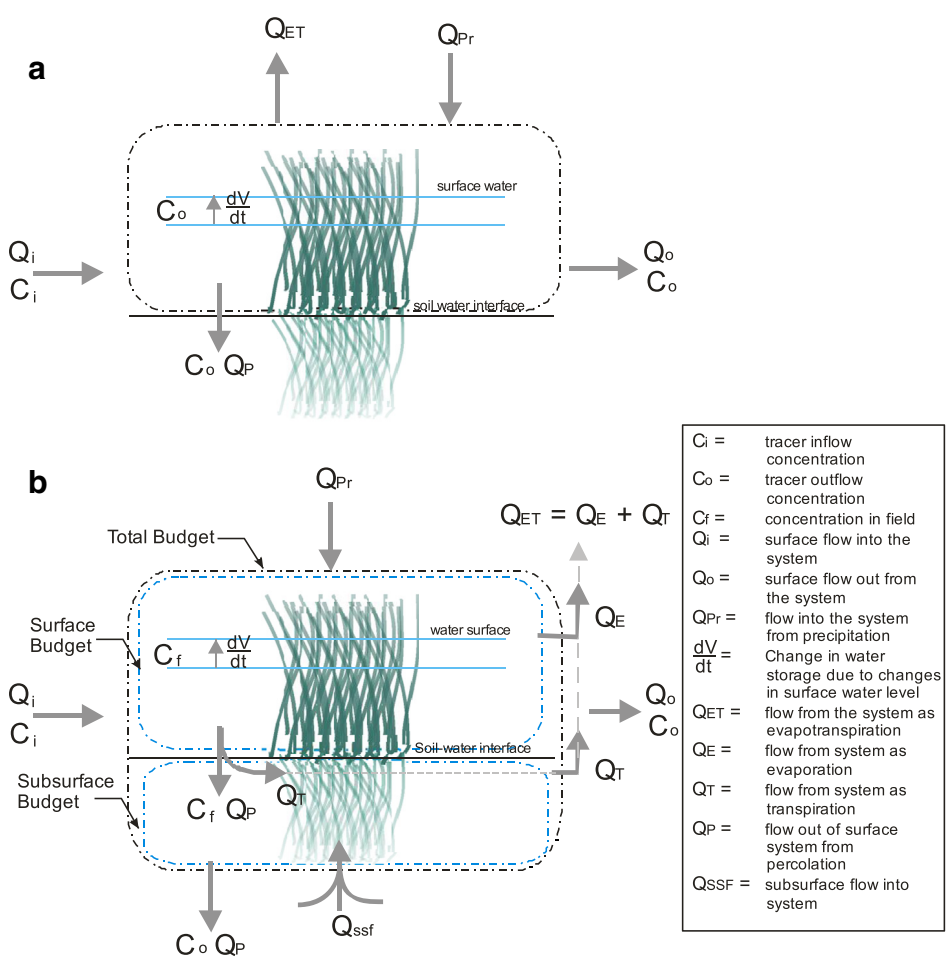

Fig. 2. Model representations showing flow paths. Loads can be lost to the surface and subsurface. Mass can be stored in the water column with increased water depths. A) Single term is used for ET (evapotranspiration), while B) ET is separated into evaporation and transpiration components and incorporates subsurface flows and mass budget divides the system into surface and subsurface components.

Please cite this article as: Bachand PAM, et al, Differentiating transpiration from evaporation in seasonal agricultural wetlands and the link to advective fluxes in the root zone, Sci Total Environ (2013), http://dx.doi.org/10.1016/j.scitotenv.2013.11.026

with minimal change in water storage. Thus, the subsurface water budget can be described by:

$$Q_{SSF} + Q_P = Q_T \quad (6)$$

where Q_T = flow out as transpiration (subsurface). Note that these water budgets separate transpiration and evaporation when describing ET:

$$Q_{ET} = Q_E + Q_T. \quad (7)$$

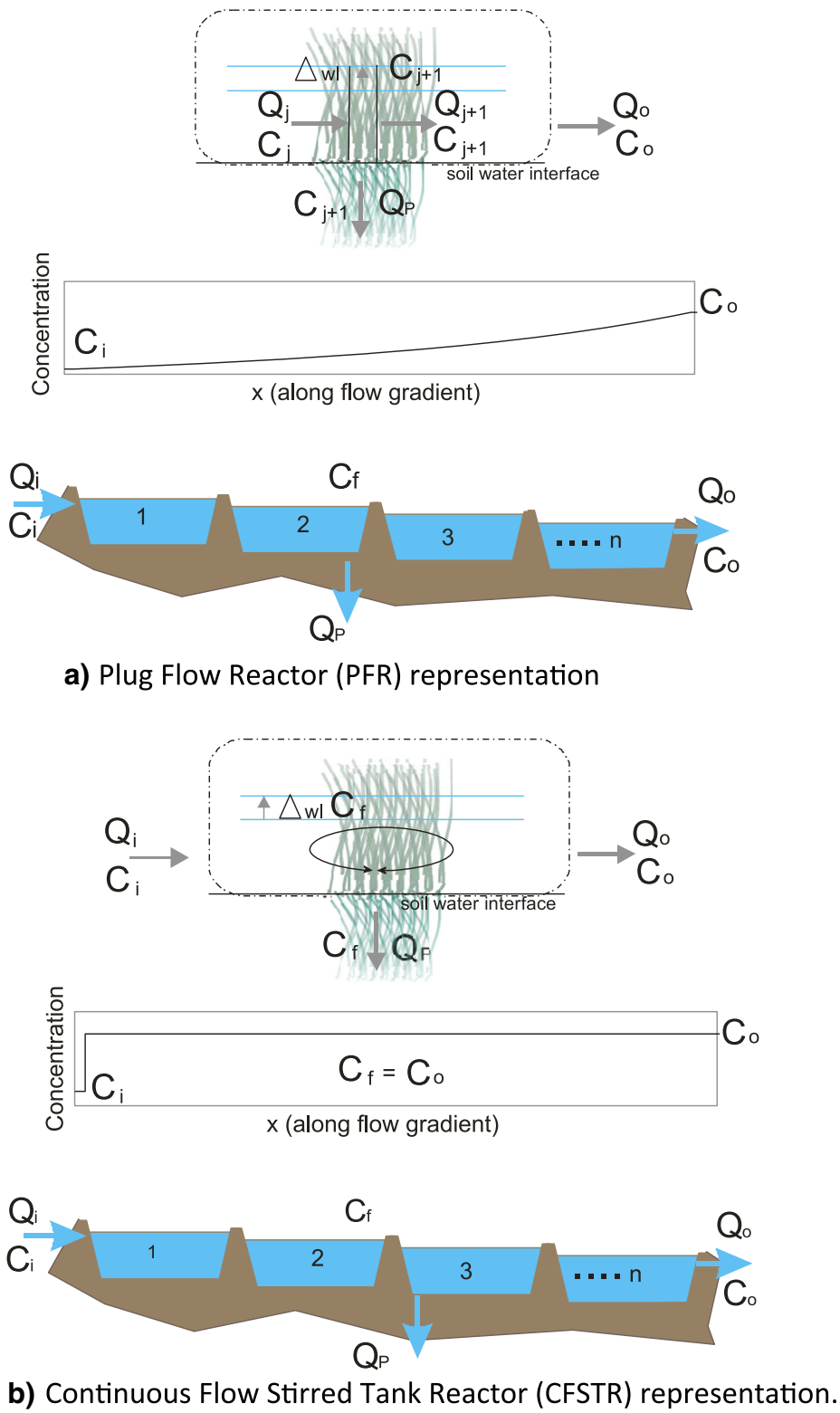

Fig. 3. Model approach diagram for sequenced check berms in agricultural wetlands. Both systems represent modeling end members. A) PFR model represents a packet of water moving through the system. B) CFSTR model represents a completely mixed condition from the inflow to outflow.

Please cite this article as: Bachand PAM, et al, Differentiating transpiration from evaporation in seasonal agricultural wetlands and the link to advective fluxes in the root zone, Sci Total Environ (2013), http://dx.doi.org/10.1016/j.scitotenv.2013.11.026

2.4.2. PFR and CFSTR framework

Next, we integrated the above model (Eqs. (3)–(7)) into a Plug Flow Reactor (PFR) and Continuous Flow Stirred Tank Reactor (CFSTR) framework. The wetland systems are partially mixed systems somewhere between two ideal solutions, the completely mixed CFSTR system to the completely unmixed PFR system (Fig. 3). We derived steady-state mass balance models for each of these to bracket the results from these wetlands. The steady-state PFR model (Fig. 3a) derived for the system assumes only linear advective transport (no mixing) and does not account for surface water dispersion or diffusion. In the PFR model, packets of water pass through the system and the concentration of the studied constituent changes as it moves through the system (Metcalf and Eddy, 2009; Tchobanoglous and Schroeder, 1985). Alternatively, the steady-state CFSTR model (Fig. 3b) has two basic assumptions: each agricultural wetland (across all the checks) is thoroughly mixed with constituent concentrations; and constituent concentration in the agricultural wetland (C_f) is equal to the outflow concentration (Metcalf and Eddy, 2009; Tchobanoglous and Schroeder, 1985). These two mass balances approaches the bookend conditions for rice from a non-mixed to a completely mixed condition. For both analyses, we used EC concentrations as the natural conservative tracer, given the regular nature of EC data collection. Further water quality data (Alpers et al., in this issue) illustrates the strong correlation of EC with Cl data ($R = 0.944$, $n = 254$ samples).

The PFR mass budget is:

$$Q_jC_j = \Delta xw\left(u_P + \frac{dh}{dt}\right)C_{j+1} + Q_{j+1}C_{j+1} \tag{8}$$

where Q_j = flow at location j along the x-gradient ($L\ s^{-1}$; direction of flow); C_j = conservative tracer (i.e. EC) concentration at location j ($mg\ L^{-1}$); Q_{j+1} = flow at location j + 1 ($L\ s^{-1}$); C_{j+1} = conservative tracer (i.e. EC) concentration at location j + 1 ($mg\ L^{-1}$); Δx = an incremental distance in the direction of flow (cm); w = the width of the agricultural wetland (cm; m); u_P = percolation rate out ($cm\ d^{-1}$); and dh/dt = rate of change in water level ($cm\ d^{-1}$). For the defined incremental area (Figs. 2b, 3a), the water budget is defined as:

$$Q_{j+1} = Q_j - \left(u_E + u_P + \frac{dh}{dt}\right)\Delta xw \tag{9}$$

where u_E = evaporation rate from surface waters ($cm\ d^{-1}$); and u_P = percolation rate ($cm\ d^{-1}$).

Combining Eqs. (8) and (9) yields:

$$Q_jC_j = Q_jC_{j+1} - \Delta xwu_EC_{j+1} \tag{10}$$

defining ΔC as C_{j+1}–C_j, and ΔQ as Q_{j+1}–Q_j leads to:

$$\frac{\Delta C}{C_{j+1}} = \frac{\Delta xwu_E}{Q_j} = -\frac{\Delta Q}{Q_j}\frac{u_E}{\left(u_E + u_P + \frac{dh}{dt}\right)}. \tag{11}$$

For steady state inflow and outflow conditions, the integral of this equation as Δx, ΔC, and ΔQ approach dx, dC, dQ yields:

$$LN\left(\frac{C_o}{C_i}\right) = -\frac{u_E}{\left(u_E + u_P + \frac{dh}{dt}\right)}LN\left(\frac{Q_o}{Q_i}\right). \tag{12}$$

This derivation assumes that evaporation, precipitation and changes in water level do not change along the x-axis, the direction of the integration. With zero precipitation and noting that $Q_E = (u_E)(Area_{HU})$, evaporative losses can be calculated by:

$$Q_E = \left(\frac{LN\frac{C_o}{C_i}}{LN\frac{Q_o}{Q_i}}\right)(Q_o - Q_i). \tag{13}$$

The CFSTR mass balance model assumes that the conservative tracer concentration in the agricultural wetland is initially the same throughout the wetland and equal to the outflow concentrations. The resulting mass budget is represented in Eq. (14):

$$C_iQ_i = C_o\left(Q_o + \frac{dV}{dt} + Q_P\right) \tag{14}$$

where C_i = conservative tracer (i.e. EC) inflow concentration; and C_o = conservative tracer (i.e. EC) outflow concentration. Combined with the surface water budget shown in Eq. (5), outflow concentration can be represented as follows:

$$C_o = C_i\left(\frac{Q_i}{Q_i + Q_{Pr} - Q_E}\right). \tag{15}$$

Evaporative losses can then be calculated:

$$Q_E = Q_i + Q_{Pr} - \left(\frac{C_i}{C_o}\right)Q_i. \tag{16}$$

2.4.3. Calculating transpiration and evaporation pathways for subset of data

Transpiration and evaporation flows were quantified using a subset of data that represented quasi-steady state conditions. Data used were from the irrigation season; an automated filter that identified quasi-steady state conditions was based on the following criteria: inflow rates were greater than zero; outflow rates were greater than zero; inflow rates were greater than outflow rates; and coincident measurements of flow, EC and water level were available. Of the 72 paired sets meeting these conditions (Table SI 1), 69 were for rice and wild rice agricultural wetlands. Fallowed agricultural wetlands F20 and F66 had only 1 and 2 paired data sets, respectively, due primarily to limited outflow events (Criteria 2). Whereas F20 and F66 had biogeochemical differences primarily associated with differences in productivity and field size (Windham-Myers et al., in this issue-a), they were hydrologically similar (e.g. Fig. SI 2) with both managed for minimum water use and thus only flooded to stimulate weed germination, resulting in very limited outflows. No irrigation data was available for the permanently or seasonally flooded wetlands. From this subset, evaporation and transpiration were calculated within the ACCESS (Microsoft Corporation 2003) database as a percent of ET for each data point. The data were averaged by agricultural wetland to calculate seasonal averages.

As the agricultural wetlands are a series of checks or ponds (Fig. 3), the PFR model was considered best representative of these. This non-ideal model configuration approaches a PFR model when complete mixing is assumed within each check or pond (Metcalf and Eddy, 2009). From the PFR relationship, we calculated the seasonal relationship between transpiration and ET rates:

$$Q_T = kQ_{ET} \tag{17}$$

where k = seasonal % of evapotranspiration rates lost by transpiration rates. This factor was integrated back into the water budget derivation discussed earlier for the hydraulic budget (Fig. 2b).

Finally, evaporation rates were compared with an independent isotope based assay of evaporation as described in Alpers et al. (in this issue). Based on a Rayleigh fractionation equation applied to surface

water (H_2O) oxygen isotope data, a shift in $\delta^{18}O$ of about 5 per mil corresponded to evaporation rates of ~50%, showing good agreement across the wide range of seasonal conditions (R = 0.805).

2.4.4. Advective and diffusive fluxes in the root zone

The estimation of transpiration enabled us to derive a relationship to compare advective and diffusive fluxes in the root zone (Fig. 4), where transpiration-driven advective flow is assumed directed downward and diffusive flow is assumed directed upward (greater concentrations of methylmercury in porewater than in the surface water column). Our goal was to determine through the flux model the transitional depth in the root zone in which fluxes change from being diffusive dominated to advective dominated. We defined this transitional depth as Z_{trans}. This derivation was developed to provide an understanding of transport in the shallow root zone similar to the understanding that is provided by the Peclet number (Pe) in groundwater (Freeze and Cherry, 1979) and surface water systems (Metcalf and Eddy, 2009):

$$Pe = \frac{uL}{D} \tag{18}$$

where L = effective length over which transport is occurring; u = velocity; and D = mass diffusion coefficient ($cm^2\ s^{-1}$; Freeze and Cherry, 1979). The Pe depends upon L; a Pe value of 1 means advection and diffusion fluxes are generally equivalent (Cushman-Roisin and Beckers, 2011), Pe > 10 signifies an advection dominated system and Pe < 0.1 signifies a diffusion dominated system. In groundwater analyses, L is typically related to grain size (Freeze and Cherry, 1979). In surface water systems, L has been identified as the length of a treatment cell. As Pe has not been defined for the wetland root zones, we derived advective and diffusive flux relationships for depths within the root zone. Flux is defined as the rate of mass movement per unit area ($cm\ s^{-1}\ mg\ L^{-1}$). Advective flux (J_A) from the water column to the root zone at the soil–water interface is calculated as:

$$J_A = C \times u_P. \tag{19}$$

Once the flow enters the pore space, downward velocity increases because the sediment water can only pass through the available pore space which reduces the area cross-section through which water can pass (Fig. 4). Thus, velocity in the pore space (u_P^{ϕ}) becomes:

$$u_P^{\phi} = \frac{u_P}{\phi}. \tag{20}$$

where ϕ = porosity (cm^3 void space cm^{-3} bulk volume). Thus, at depth z within the pore space, the flux at that location when described as per unit area of pore or void space becomes:

$$J_{A,z}^{\phi} = C_z \frac{u_P}{\phi}. \tag{21}$$

Diffusive flux can be calculated by Fick's First Law:

$$J_D = -D\frac{dC}{dz}. \tag{22}$$

We used mass diffusion coefficients based upon the literature for Hg (Gill et al., 1999; Langer et al., 2001; Holmes and Lean, 2006). Integrating along the z-axis from a depth Z to the soil–water interface, we assumed a linear concentration along the gradient and assumed tortuosity (θ; length of the curve compared to the distance between the curve ends) follows the relationship $\theta^2 = \sqrt{1 - \ln\left(\phi^2\right)}$ (Bourdreau, 1996). Upward diffusive flux at depth z within the pore space becomes:

$$J_{D,z}^{\phi} = -D\frac{C_z - C_F}{z\theta} \tag{23}$$

where $z\theta$ = the length over which diffusion occurs. To identify the transitional depth (Z_{trans}) at which flux transport moves from diffusive to advective dominated transport, we first summed these to fluxes to calculate the total flux through the root zone ($J_{T,z}^{\phi}$):

$$J_{T,z}^{\phi} = J_{A,z}^{\phi} + J_{D,z}^{\phi} \tag{24}$$

At $J_{T,z}^{\phi} = 0$ advective flux and diffusive flux cancel each other out and this condition is used to calculate Z_{trans}. The greatest upward diffusive flux would occur when concentrations of the constituent in the water

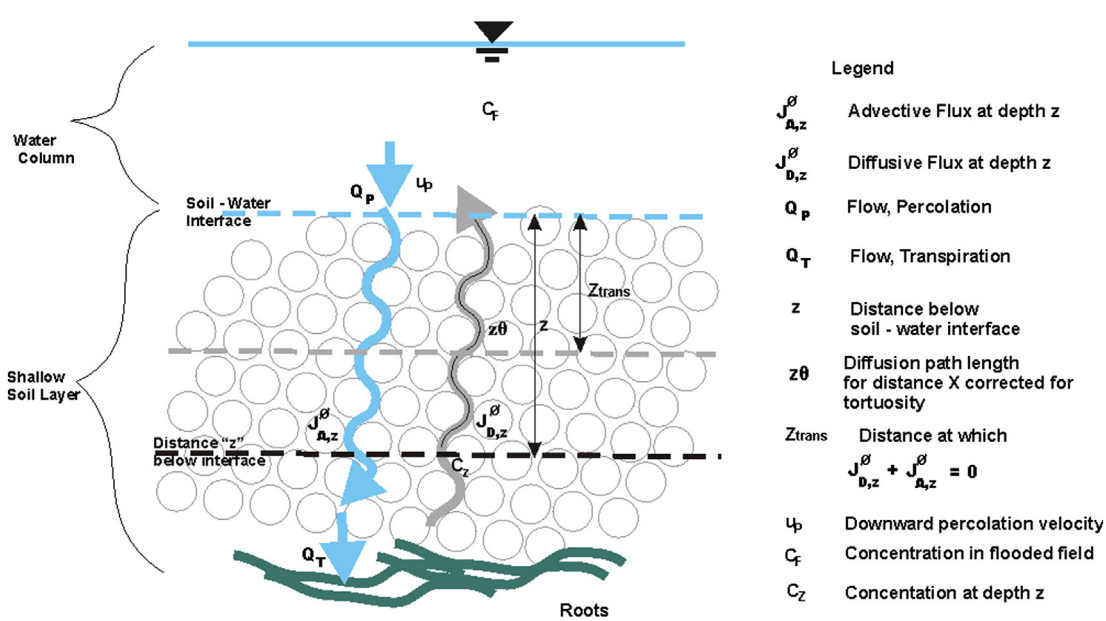

Fig. 4. Root zone model. Formulas for advective and diffusive fluxes are developed based upon the root zone model and these formulas are integrated into a root zone mass balance. The mass balance is used to characterize the critical depth into the shallow root zone in which transport transitions from diffusive to advective transport.

Please cite this article as: Bachand PAM, et al, Differentiating transpiration from evaporation in seasonal agricultural wetlands and the link to advective fluxes in the root zone, Sci Total Environ (2013), http://dx.doi.org/10.1016/j.scitotenv.2013.11.026

column are negligible ($C_F = 0$). Under these conditions, zero flux can be described by the following equation:

$$0 = J^{\phi}_{A,z} + J^{\phi}_{D,z} = C_z \frac{u_P}{\phi} - D \frac{C_z}{Z_{trans}\theta}. \quad (25)$$

This can be furthered simplified to:

$$\frac{u_P}{\phi} = \frac{D}{Z_{trans}\theta}. \quad (26)$$

The transition depth below which advection dominates becomes:

$$Z_{trans} = \frac{\phi}{\theta}\frac{D}{u_P} = \frac{\phi}{\sqrt{(1 - \ln(\phi^2))}}\frac{D}{u_P}, \quad (27)$$

similar to the Pe equation. If transpiration is the only driver of percolation, the transition depth due to transpiration $Z_{trans,T}$ becomes:

$$Z_{trans,T} = \frac{\phi}{\theta}\frac{D}{u_T}. \quad (28)$$

2.5. Data analyses and QAQC

All data were compiled in Microsoft® ACCESS (Microsoft Corporation 2003). Database tools (e.g. pivot tables and graphs, queries) were developed to identify and correct quality assurance and quality control (QAQC) problems associated with the varied and different data sets (i.e. lab analyses, inconsistencies or errors in data entry, outliers). ACCESS was also used to consolidate, integrate and synchronize data for each agricultural wetland: summing flows at weirs to determine total inflow or outflow for agricultural wetlands with multiple inflows or outflows; calculating water level changes based upon outflow staff gauge readings; incorporating California Irrigation Management Information System (CIMIS) data with crop coefficients to provide temporal ET data for each agricultural wetland; developing water and mass budgets for each discrete sampling date. Hydrologic and water quality trends and statistical significance for the different cropping treatments were conducted using Statistica (StatSoft Inc. 2008). All data are reported as means and standard errors, unless otherwise noted.

2.6. Uncertainty related to farm management

Because the study was performed alongside unmodified farm operations, agricultural wetland conditions generated multiple sources of uncertainty related to farm management. Agronomic needs controlled irrigation practices, and researchers only monitored hydrologic and water quality data (Windham-Myers et al., in this issue-a). Because of this management, flow conditions over the weirs were not always met and could not be managed to reduce hydrologic sources of error. Surface water depths were estimated by linking water elevation data at HU outflow weirs with average water depth data from HU centers. Agricultural wetlands were sequentially flooded over a two to three week period, resulting in some differences within cropping types regarding inundation. Also, different cropping types were flooded for different periods of time (rice > wild rice > fallowed agricultural wetlands). Finally, some model uncertainty resulted from evapotranspiration K_c values. Values used to calculate evapotranspiration needed to be estimated for some crops as they are not available. These estimates, based on leaf area (Frank Anderson, USGS unpublished data), predominantly occurred outside the growing season. These sources of error create some uncertainty and data gaps with water budgets, particularly over entire seasons, and define periods of time during which EC mass balances could be applied. These sources of error were outside the control of researchers and common in studies of real-world systems.

3. Results

3.1. Hydrology

The irrigation season hydrologic data which provide the basis for the water and mass balance analyses and for model calculations are inflow and outflow magnitudes (Fig. SI 5), ET and changes in water depth during the seasons (Figs. SI 5, SI 2). Flows along the different pathways (e.g. surface inflow, surface outflow, transpiration, evaporation) were quantified throughout the year. During the irrigation season, inflow Hydraulic Loading Rates (HLRs) varied temporally from 0 to 3 cm d^{-1} (Fig. SI 5) averaging 1.14 ± 0.07 cm d^{-1} across all the agricultural wetlands between early June and mid-September. Inflow HLR changes occurred both gradually over a few weeks, but were also subject to daily pulses based on agricultural management. Initial loading rates were more rapid in rice and wild rice (2.5 to 5.5 cm d^{-1}) than fallow agricultural wetlands but all rates lowered after flood conditions were obtained (0.5 to 2 cm d^{-1}).

Regardless of the different inflow conditions during the summer, outflow HLRs were generally low (0.0 to 1.0 cm d^{-1}, Fig. SI 5) and significantly lower from inflow HLRs ($p = 0.0000$; T-test for Dependent Samples, Statsoft (2008)). Only during rapid pre-harvest drainage event in rice agricultural wetlands were outflow HLRs higher than inflow HLRs. Fallowed agricultural wetlands generally had no outflow during periods in which they were flooded. Rice agricultural wetlands had more variable outflow HLRs, ranging from 0.0 to over 1.0 cm d^{-1}. Wild rice agricultural wetlands generally had outflows between 0.0 and 0.5 cm d^{-1}.

Each crop type resulted in different ET trends through the year due to a number of factors. Flooding resulted in sharp K_c increase (Fig. SI 4) for all agricultural wetlands, subsequently declining in response to plant shading and flattening out to 1.10 for rice and 1.05 for wild rice as the crops matured. As shown in Fig. SI 2, ET for each agricultural wetland began declining late in the irrigation season as a result of plant senescence, draining, and shorter days. ET decreased in September and October as the fall equinox approached and passed. Rice and wild rice had similar ET trends due to similar management. In comparison, the fallowed agricultural wetlands had higher ET in the late spring due to weed establishment and had delayed and shortened summer ET rates because of delayed and shortened inundation periods. In general, modeled ET rates replicated well within the crop types (Fig. SI 2).

The reference evapotranspiration (ET_o) also affected ET rates; the non-agricultural wetlands had ET rates that more closely tracked ET_o because of the continual establishment of vegetation: ET total rates in permanent wetland were 25% higher than in seasonal wetland due to year-round inundation.

Winter flooding was more spatially uniform than summer flooding for all the agricultural wetlands (Fig. SI 6): agricultural wetlands were flooded in late November, water depths were approximately 20–30 cm (Fig. SI 6) and then in January water levels increased dramatically as the wetlands transitioned from water management primarily for wildlife and to water management primarily for flood control (Table SI 1).

3.2. Hydrologic and tracer budgets to quantify evaporation and transpiration rates

Hydrologic and tracer mass budgets were developed for a subset of quasi-steady state data to separate transpiration and evaporation. Table 1 provides the data and results of the hydrologic balance for both the PFR and CFSTR models. During the summer flooding period, electrical conductivity (EC) was significantly greater in the outflows than in the inflows throughout the summer flooding period (Fig. SI 7). Electrical conductivity typically increased 2-to-3 fold through the summer, indicating evaporative losses. Inflow HLRs averaged 1.14 ± 0.07 cm d^{-1} across all the agricultural wetlands, with averages ranging from 0.65 to 1.43 cm d^{-1} for the different wetlands (Table 1). Outflow HLRs were

Table 1
Hydrologic inputs and outputs by agricultural wetlands for early June through mid-September 2007 when data met PFR and CFSTR model requirements. PFR = plug flow reactor, CFSTR = continuous flow stirred tank reactor, HLR_i = inflow hydraulic loading rate, HLR_o = outflow HLR, u_p = percolation rate, u_{SSF} = flow rate from subsurface, u_T = transpiration loss (subsurface), dh/dt = increase in surface water elevation.

Total budget [1,2,3,4]											
	HLR_i (in)		u_{ssf} (in)[5]		HLR_o (out)		u_{ET} (out)		dh/dt [7]		
	Mean	SE	Mean	SE	Mean	SE	Mean	SE	Mean	SE	N[6,8]
F20	*1.38*	*0.57*	*−0.20*	*1.33*	*0.01*	*0.28*	*0.65*	*0.10*	*0.52*	*1.22*	*1*
F66	*0.65*	0.40	*−0.22*	*0.94*	*0.10*	*0.20*	*0.59*	*0.07*	*−0.26*	*0.86*	*2*
R31	0.98	0.15	−0.04	0.35	0.27	0.08	0.64	0.03	0.02	0.33	14
R64	1.43	0.13	−0.05	0.30	0.49	0.06	0.65	0.02	0.23	0.27	20
W32	1.16	0.13	−0.46	0.31	0.38	0.07	0.70	0.02	−0.38	0.29	18
W65	0.97	0.14	−0.39	0.32	0.16	0.07	0.70	0.02	−0.28	0.30	17
All	1.14	0.07	−0.24	0.15	0.33	0.04	0.67	0.01	−0.09	0.14	72
Surface water budget											
CFSTR											
	HLR_i (in)		u_{ssf} (in)[5]		HLR_o (out)		u_{ET} (out)		dh/dt [7]		
	Mean	SE	Mean	SE	Mean	SE	Mean	SE	Mean	SE	N[6,8]
F20	*1.38*	*0.57*	*0.07*	*1.26*	*0.01*	*0.28*	*0.78*	*0.18*	*0.52*	*1.22*	*1*
F66	*0.65*	*0.40*	*0.51*	*0.89*	*0.10*	*0.20*	*0.30*	*0.13*	*−0.26*	*0.86*	*2*
R31	0.98	0.15	0.43	0.34	0.27	0.08	0.25	0.05	0.02	0.33	14
R64	1.43	0.13	0.22	0.28	0.49	0.06	0.49	0.04	0.23	0.27	20
W32	1.16	0.13	0.87	0.30	0.38	0.07	0.29	0.04	−0.38	0.29	18
W65	0.97	0.14	0.75	0.30	0.16	0.07	0.34	0.04	−0.28	0.30	17
All	1.14	0.07	0.55	0.15	0.33	0.04	0.36	0.02	−0.09	0.14	72
PFR											
	HLR_i (in)		u_{ssf} (in)[5]		HLR_o (out)		u_{ET} (out)		dh/dt [7]		
	Mean	SE	Mean	SE	Mean	SE	Mean	SE	Mean	SE	N[6,8]
F20	*1.38*	*0.57*	*0.64*	*1.27*	*0.01*	*0.28*	*0.21*	*0.13*	*0.52*	*1.22*	*1*
F66	*0.65*	*0.40*	*0.65*	*0.90*	*0.10*	*0.20*	*0.16*	*0.09*	*−0.26*	*0.86*	*2*
R31	0.98	0.15	0.54	0.34	0.27	0.08	0.14	0.04	0.02	0.33	14
R64	1.43	0.13	0.34	0.28	0.49	0.06	0.37	0.03	0.23	0.27	20
W32	1.16	0.13	0.97	0.30	0.38	0.07	0.19	0.03	−0.38	0.29	18
W65	0.97	0.14	0.90	0.31	0.16	0.07	0.19	0.03	−0.28	0.30	17
All	1.14	0.07	0.68	0.15	0.33	0.04	0.23	0.02	−0.09	0.14	72
Subsurface water budget											
CFSTR											
	u_p (in)		u_{ssf} (in)		u_T (out)						
	Mean	SE	Mean	SE	Mean	SE	N[6,8]				
F20	*0.07*	*1.26*	*−0.20*	*1.33*	*−0.13*	*0.21*	*1*				
F66	*0.51*	*0.89*	*−0.22*	*0.94*	*0.29*	*0.15*	*2*				
R31	0.43	0.34	−0.04	0.35	0.39	0.06	14				
R64	0.22	0.28	−0.05	0.30	0.16	0.05	20				
W32	0.87	0.30	−0.46	0.31	0.41	0.05	18				
W65	0.75	0.30	−0.39	0.32	0.36	0.05	17				
All	0.55	0.15	−0.24	0.15	0.31	0.03	72				
PFR											
	u_p (in)		u_{ssf} (in)		u_T (out)						
	Mean	SE	Mean	SE	Mean	SE	N[6,8]				
F20	*0.64*	*1.27*	*−0.20*	*1.33*	*0.44*	*0.17*	*1*				
F66	*0.65*	*0.90*	*−0.22*	*0.94*	*0.43*	*0.12*	*2*				
R31	0.54	0.34	−0.04	0.35	0.50	0.05	14				
R64	0.34	0.28	−0.05	0.30	0.28	0.04	20				
W32	0.97	0.30	−0.46	0.31	0.51	0.04	18				
W65	0.90	0.31	−0.39	0.32	0.51	0.04	17				
All	0.68	0.15	−0.24	0.15	0.44	0.02	72				

Notes

1. Shaded cells of different colors show values differed significantly from each other, *(Tukey Unequal N HSD).*
2. Values in cm/d.
3. Mean conductivity of inflow water = 986 uS/cm (SD=190; SE=22).
4. Mean conductivity of outflow water = 1463 (SD=327, SE=38)
5. Value calculated using budget. Positive when subsurface flow up into root zone.
6. N is number of data pairs for which all data is complete.
7. Change in water level (storage) is positive when water level is increasing.
8. *Data in itallics are for fields with limited data*

significantly lower ($p = 0.0000$; T-test for Dependent Samples; Statsoft, 2008), averaging 0.33 ± 0.04 cm d^{-1} with a range of 0.0 to 1.0 cm d^{-1} for the different wetlands. Under the PFR model, evaporation calculations resulted in an average of 0.23 ± 0.02 cm d^{-1}, ranging from 0.14 to 0.21 cm d^{-1} for all agricultural wetland except for R64. Wetland R64 had statistically greater evaporation than the other

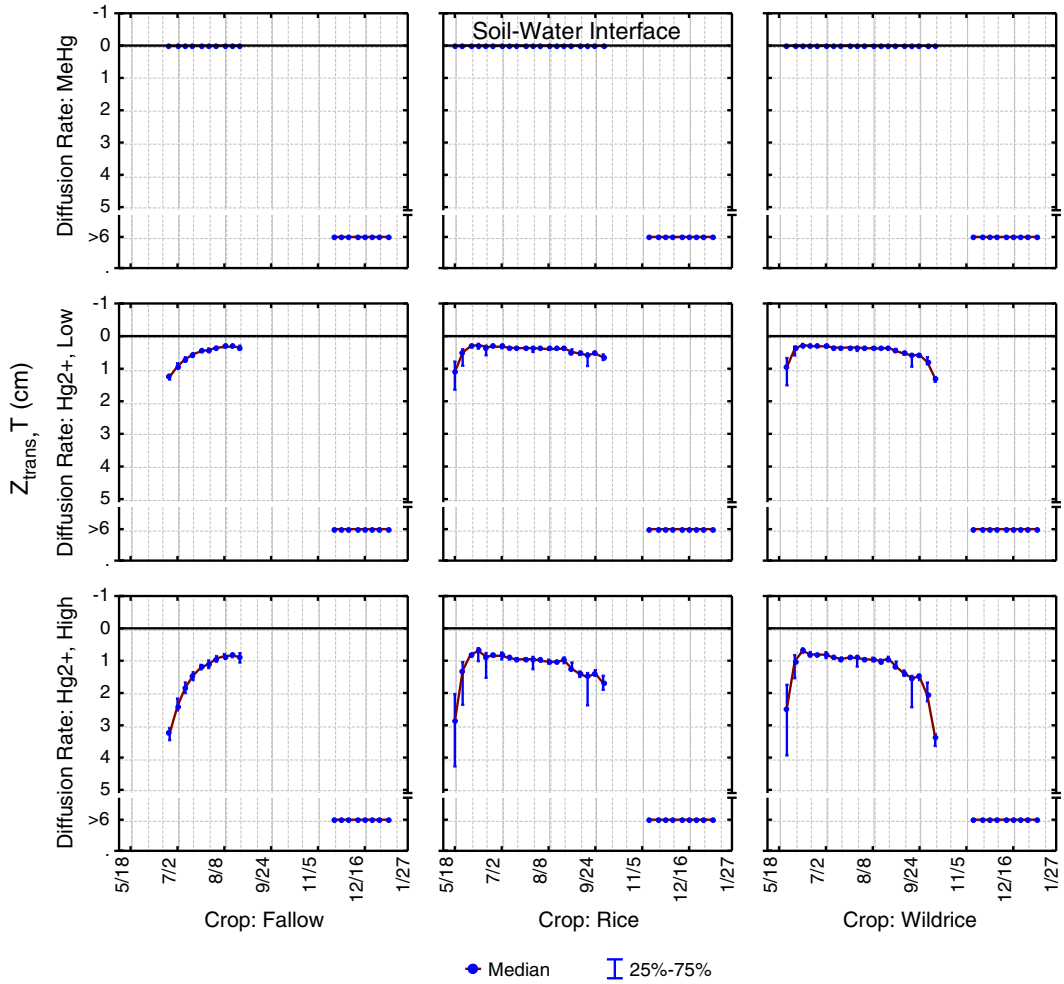

Fig. 5. Monthly changes in transition depth for Hg diffusion rates in the shallow root zone. Diffusion rates are based upon published literature on concentrations for a) MeHg, b) low range for inorganic Hg, and c) high range for inorganic Hg. The transition depth Z_{trans} is an estimate of the depth in the root zone at which transport and fluxes change from diffusion dominated (above Z_{trans}) to advection dominated (below Z_{trans}). During the months in which transpiration is occurring for these crops (June through September), advective fluxes are the main transport mechanism in all but the upper centimeters or fraction of centimeters. During this period, diffusion only dominates in the upper layer of the root zone. When transpiration ceases, advection ceases to and diffusion drives fluxes in the shallow root zone.

agricultural wetlands (0.37 ± 0.03 cm d^{-1}; Table 1). Calculated percolation rates averaged 0.68 ± 0.15 cm d^{-1} (range = 0.34–0.97 cm d^{-1}), with the highest rates observed in R64. Calculated transpiration rates averaged 0.44 ± 0.02 cm d^{-1} among agricultural wetlands. Agricultural wetland R64 had statistically lower rates of transpiration (0.28 ± 0.04 cm d^{-1}, $p < 0.0001$) than the other three cropped agricultural wetlands (0.51 ± 0.01 cm d^{-1}). For the CFSTR model, evaporation rate calculations averaged 0.36 ± 0.02 cm d^{-1} for all agricultural wetlands (range = 0.25–0.49 cm d^{-1} for rice and wild rice agricultural wetlands). Significant differences ($p < 0.0001$) in calculated evaporation rates between agricultural wetlands were attributed to R64 as compared to R31 and W32 (Tukey Unequal N HSD, StatSoft Inc. 2008). Calculated percolation rates averaged 0.55 ± 0.15 cm d^{-1} (range = 0.07–0.87 cm d^{-1}). The transpiration rates calculated with the CFSTR model averaged 0.31 ± 0.03 cm d^{-1} (range = 0.16–0.41 cm d^{-1}) for the cropped agricultural wetlands. As with the PFR model, transpiration rates were lower in R64 (0.16 ± 0.05 cm d^{-1}) than the other cropped agricultural wetlands (0.38 ± 0.03, $p < 0.00006$).

Wetland R64 accounted for most of these differences with regard to calculated transpiration. This wetland was the only agricultural wetland to be drained and flooded again during the development period of these calculations (Table SI 1) and perhaps those actions compromised analyses with regard to quasi-steady state conditions and management and operational uncertainty.

Table SI 4 summarizes the modeling results across all agricultural wetlands during this time period except for R64. The PFR model predicted percolation rates of 0.81 ± 0.17 cm d^{-1}, transpiration losses of 0.50 ± 0.02 cm d^{-1} and evaporation losses of 0.18 cm d^{-1}. In comparison, the CFSTR analysis predicted lower mean percolation rates of about 0.68 ± 0.07 cm d^{-1}, lower transpiration rates of 0.37 ± 0.03 cm d^{-1}, and higher evaporation rates of 0.30 ± 0.03 cm d^{-1}. Thus when R64 is not included, the PFR model predicts transpiration as 74% of evapotranspiration and the CFSTR model predicts 55%.

3.3. Water budget: spring through fall

Table SI 5 provides a water budget for the different agricultural wetlands for spring through fall, using all available data for those seasons. The results of this water budget are graphically displayed in Fig. 1, showing the development of soil water deficits, periods of irrigation and winter flooding. In water budget calculations, winter was not included as flows are unconstrained during most of the winter season. Based upon the PFR model results, transpiration was estimated as 75% of ET during the irrigation season. During spring and fall, transpiration was assumed to be negligible due to the absence of plants (spring) and senescence (fall). During the irrigation season, irrigation water accounted for nearly all water onto the agricultural wetlands during the irrigation period: 37–50 cm applied to the fallow agricultural

ARTICLE IN PRESS

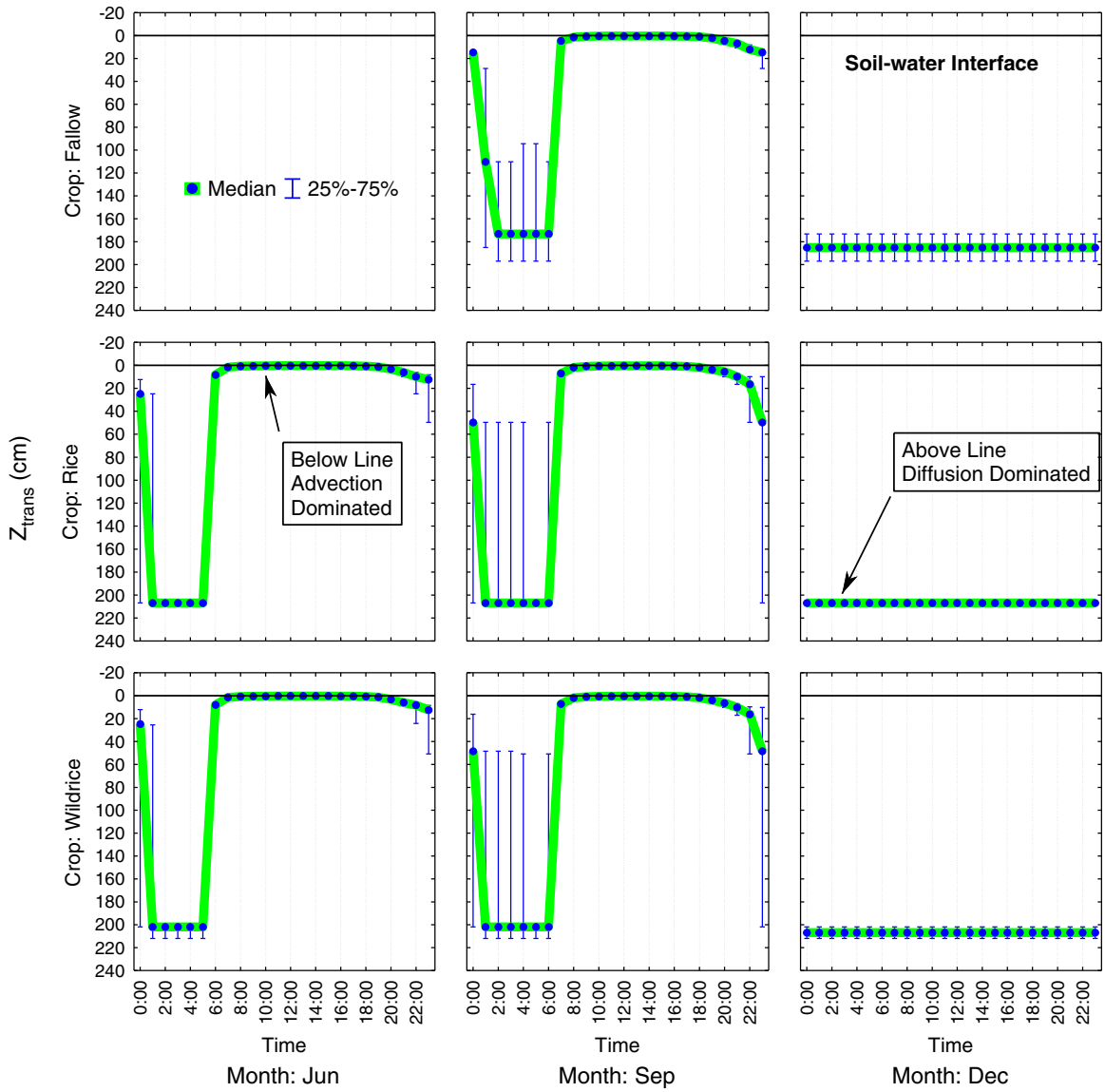

Fig. 6. Diel transition depth changes in the shallow root zone for the different agricultural wetland crops during June, September and December for high Hg^{2+} diffusion rates. Diel variations in transpiration result in diel changes in the transition depth. The transition depth is an estimate of the depth in the root zone at which transport and fluxes change from diffusion dominated (above Z_{trans}) to advection dominated (below Z_{trans}). Thus, during the period of the day when transpiration is occurring, advective fluxes are the main transport mechanism in the root zone. This can be seen during those months when transpiration is occurring, such as June and September. When transpiration is not occurring, diffusive fluxes dominate throughout the root zone.

wetlands, 102–137 cm applied to the rice and wild rice agricultural wetlands. Evapotranspiration accounted for most of the water losses from irrigation: 78–89 cm for rice and wild rice and about 43 cm for fallowed agricultural wetlands. Only 15% of irrigation waters were discharged as surface outflows for fallowed agricultural wetlands (6 cm), and only 15–31% for rice and wild rice agricultural wetlands (16–43 cm). The irrigation season was marked by high ET rates on the order of 0.5 to almost 1.2 cm d^{-1}.

3.4. Transpiration driving subsurface fluxes

Transpiration and evaporation rates (Figs. SI 8; SI 9) were based upon the assumption that these systems are best modeled as PFRs. Transpiration and evaporation rates are calculated using Eq. (17), which multiplies ET rates by "k", seasonal % of evapotranspiration rates lost by transpiration rates. Monthly percolation rates have large error bars (Fig. SI 8) likely resulting in part from methodology used to calculate percolation in the context of wetland operation. The hydrology of these systems varies temporally in response to management. Data from these systems lag in response to changes in operation and this lag propagates through the hydrologic balance, causing variance in percolation rate calculations.

Evaporation was fairly constant throughout the year. Thus, seasonal transpiration trends (Fig. SI 8) track seasonal ET trends (Fig. SI 2) and diel transpiration trends can be calculated from diel evapotranspiration trends as well (Fig. SI 10). These transpiration trends drive percolation patterns during much of the year which is demonstrated in the hydrologic balance calculations (Figs. SI 8, SI 9). Fig. SI 9 shows the ratio of percolation rates to transpiration rates for data under relatively steady state hydrologic conditions: inflow hydrologic rates and outflow rates greater than 0 cm d^{-1} and water level changes less than 0.1 cm d^{-1}.

Percolation rates were predicted from transpiration rates during much of the irrigation season (Fig. SI 8). An exception is during initial flood periods when the root zone soils become saturated and percolation rates are higher as surface water moves into the unsaturated pore spaces. Under those conditions, this ratio approaches 1 for much of the irrigation season. During July in which the system is under quasi-steady state conditions with regard to water management and evaporation rates,

Please cite this article as: Bachand PAM, et al, Differentiating transpiration from evaporation in seasonal agricultural wetlands and the link to advective fluxes in the root zone, Sci Total Environ (2013), http://dx.doi.org/10.1016/j.scitotenv.2013.11.026

Table 2
Evapotranspiration assumption effects on hydrologic and mass budgets. Four scenarios are presented below using average input data from this study. Scenarios 1 & 2 assume different reactor models and that assumption affects calculated values of percolation, transpiration and evaporation rates. Scenarios 3 & 4 use the CFSTR model for convenience, treat evapotranspiration as an evaporation pathway, and assume an incomplete data set (outflow EC for Scenario 3, outflow HLR for Scenario 4). The calculations in scenarios 3 & 4 determine that the missing data differ greatly from actual data from the study and demonstrate how misrepresenting evapotranspiration hydrologic pathways will greatly skew resulting calculations.

Scenario	1		2		3		4	
Assumed reactor model	PFR		CFSTR		CFSTR[a]		CFSTR[a]	
Evapotranspiration pathways	ET separated into evaporation and transpiration pathways				ET treated as evaporation pathway			
Missing data	Data complete		Data complete		Conductivity at outflow		ET and Qo unknown	
Mass budget[b]								
HLR_i (cm/d)	1.03	i	1.03	i	1.03	i	1.03	i
u_{ssf} (cm/d)	−0.31	c	−0.31	c	−0.31	c	−0.31	c
HLR_o (cm/d)	0.26	i	0.26	i	0.26	i	*0.62*	c
dh/dt (cm/d)[c]	−0.22	i	−0.22	i	−0.22	i	−0.22	i
EC_{in}, μS/cm	998	i	998	i	998	i	998	i
EC_{out}, μS/cm	1455	i	1455	i	*5259*	c	1455	i
Surface water budget[b]								
HLR_i (cm/d)	1.03	i	1.03	i	1.03	i	1.03	i
HLR_o (cm/d)	0.26	i	0.26	i	0.26	i	*0.62*	i
u_P (cm/d)	0.81	c	0.68	c	*0.31*	c	*0.31*	c
u_E (cm/d)	0.18	c	0.30	c	*0.68*	c	*0.68*	c
dh/dt (cm/d)[c]	−0.22	i	−0.22	i	−0.22	i	−0.22	i
Subsurface water budget[b]								
u_p (cm/d)	0.81	c	0.68	c	*0.31*	c	*0.31*	c
u_{ssf} (cm/d)	−0.31	c	−0.31	c	−0.31	c	−0.31	c
u_T (cm/d)	0.50	c	0.37	c	*0.00*	c	*0.00*	c
ET Breakdown[b]								
u_E (cm/d)	0.18	c	0.30	c	*0.68*	c	*0.68*	c
u_T (cm/d)	0.50	c	0.37	c	*0.00*	c	*0.00*	c
u_{ET} (cm/d)	0.68	i	0.68	i	0.68	i	0.68	i
Percent of ET[b]								
uE (cm/d)	26%	c	45%	c	*100%*	a	*100%*	a
u_T (cm/d)	74%	c	55%	c	*0%*	a	*0%*	a

Notes
[a] Values underlined and in italics are resulting calculations based upon inaccurate assumptions regarding E & T.
[b] Considered positive in budget when water level/storage is increasing.
[c] Data source: I = input, measured; c = calculated; a = assumed.

percolation rates averaged 0.65 cm d^{-1} and transpiration rates averaged 0.56 cm d^{-1}. Calculation errors also affect this calculated relationship, such as when complete water or mass balance calculations cannot be made because of missing data, or during periods when large changes in water levels from farm manipulations skew hydrologic balance calculations.

Once transpiration ceases in late fall, percolation stops and even reverses (Fig. SI 8). Potential reasons for this calculated reverses in percolation rates could be 1) errors associated in changes in water level or 2) actual infiltration from elevated water levels throughout the system promoting upward subsurface flow (e.g. upwelling) in the Yolo Bypass as would occur in a gaining reach within a riverine system.

Our model in Fig. 4 predicts that transpiration leads to an advective flux into the shallow root zone from the water column. This effect would be expected to lead to a transitional depth which delineates areas in the root zone in which diffusion dominates pore water flux from areas in which advection dominates pore water flux. Similar to how the Peclet number is used to differentiate areas of diffusive transport from advective transport for surface and groundwater systems (Cushman-Roisin and Beckers, 2011, Freeze and Cherry, 1979) our flux model results (Eq. (28)) determine Z_{trans}, the depth into the root zone that flux is transitioning from diffusive flux (above Z_{trans}) to advective flux (below Z_{trans}).

The seasonally changing transpiration rates result in a seasonal migration of Z_{trans} (Fig. 5). With the beginning of flooding and plant establishment, Z_{trans} for inorganic Hg^{2+} migrates upward from between 1 and 4 cm to between 0.2 and 1 cm. These calculations utilize diffusion rates for inorganic Hg ranging from 5 to 13×10^{-6} cm^2 s^{-1} (0.4–1.1 cm^2 d^{-1}; Holmes and Lean, 2006; Gill et al., 1999). Heirn (1996) used benthic chambers to determine the diffusion rate of MeHg at two orders of magnitude lower at 4×10^{-8} cm^2 s^{-1}. This results in Z_{trans} to be calculated as two orders of magnitude lower as well. In the winter when transpiration ceases but the agricultural wetlands are still flooded, advection essentially stops throughout the root zone. Z_{trans} goes to infinity, meaning the root zone becomes diffusion dominated throughout.

Similarly, diel patterns emerge for Z_{trans} (Fig. 6) in response to diel changes in transpiration (Fig. SI 10). Diffusion dominates flux throughout the shallow root zone during the evening hours during the summer, but transpiration begins near sunrise and occurs throughout the day resulting in the upward migration of Z_{trans} such that during midday advection dominates flux throughout the soil column (Fig. 6). As summer progresses during the irrigation season, longer nights lead to longer periods of diffusion dominating flux throughout the soil column. Diel migration of Z_{trans} ceases with plant harvest and the cessation of transpiration and ET. Z_{trans} is constituent dependent, depending upon the diffusivity coefficient for the particular dissolved constituent.

4. Discussion

4.1. Calculating transpiration with natural tracers and the PFR model

In this study, we developed CFSTR and PFR relationships that enable transpiration to be calculated in wetland systems. Our calculations use EC as a natural tracer (Hayashi et al., 1998; Pellerin et al., 2007) and compare well with reported values from other methods (Kiendl, 1953; Burian, 1973; Shuttleworth and Wallace, 1985; Herbst and Kappen, 1999; Sanchez-Carrillo et al., 2004; Bouman et al., 2005). Utilizing EC, a constituent easily measured, as a natural tracer in a mass balance and integrating that calculation with a hydrologic balance represents a novel approach to quantify transpiration rates. This new approach requires that flow and natural conservative tracer data are available and

that the system is operated under quasi-steady state conditions for the period when calculations are made. Although Br is commonly used as a tracer in these types of systems (Howes et al., 1986; Whitmer et al., 2000; Parsons et al., 2004), chloride and EC are natural tracers as well. Independent cross validation between modeled evaporation, as well as seasonal and within field variability in EC concentrations, chloride concentrations and isotopic evidence of evaporation fractionation ($\delta^{18}O$) provides support for model implementation (Alpers et al., in this issue).

The CFSTR and PFR models provide end members for agricultural wetland systems, modeling from a completely mixed (CFSTR) to a non-mixed (PFR) condition. For rice and wild rice systems, the configuration of several completely mixed ponds or basins in series approaches a PFR model (Metcalf and Eddy, 2009), especially as dense vegetation in July and August (stem density average for rice = 571 +/− 33 SD) limits mixing within checks (Windham-Myers et al., in this issue-c). Using the PFR model and excluding field R64, we estimated average evaporation from 0.14 to 0.21 cm d^{-1} (21–32% of ET, average 26%) and transpiration from 0.41 to 0.51 cm d^{-1} (68–79% of ET, average 74%), which are similar to ranges calculated by others.

4.2. Why transpiration matters — getting water and mass budgets right

As discussed in the introduction, transpiration plays an important role in moving constituents from the water column into the root zone in shallow aquatic systems (Howes et al., 1986; Hayashi et al., 1998; Whitmer et al., 2000; Parsons et al., 2004; van der Kamp and Hayashi, 2009). Transpiration has been reported to have diel effects on infiltration in wetlands (Dacey and Howes, 1984) and diel and seasonal effects on seepage in lakes (Rosenberry et al., 2013). Though methods exist to directly or indirectly determine evaporation and transpiration rates separately in agricultural wetlands (Bethune et al., 2001; Bouman et al., 2005, 2007), most wetland studies aggregate these two terms into an ET rate (Mitsch and Gosselink, 1993; Kadlec and Knight, 1996; Kadlec, 2000; Bethune et al., 2001; Carleton et al., 2001; Martinez and Wise, 2003; Playan et al., 2008). Failing to recognize and quantify the importance of root uptake in ET determinations may introduce errors in load and export calculations.

Table 2 is used to illustrate this point. Scenarios 1 and 2 show calculated mass and water budgets under the PRF and CFSTR models respectively using average data values from this study for inflow and outflow HLR, changes in water elevation, ET and inflow and outflow EC. In Scenarios 1 and 2, the reactor models are assumed and all other budget data not collected from the study are calculated. The assumption of PFR and CRSTR model affects calculated percolation rates (u_p), the evaporation and transpiration rates, and their percent of total evapotranspiration. The PFR model allocates greater hydrologic transport transpiration as compared to the CFSTR model, and thus results in higher percolation rates into the root zone.

Scenarios 3 and 4 represent scenarios in which some data are considered not available and the CFSTR model is used to fill in the data with evapotranspiration being treated as an evaporation pathway. For the purpose of calculations, evaporation rates are essentially more than double their actual value, and transpiration rates are assumed as zero. The CFSTR model is used in this illustration because it provides simpler calculations than the PFR model. In Scenario 3, outflow EC levels are considered missing. Using the CFSTR model, outflow concentrations are calculated at over three times their real value. Because transpiration is not considered as its own pathway, percolation rates into the root zone are calculated as less than half of the calculated values in Scenario 2. In Scenario 4, outflow rates are considered missing. With the same CRSTR model and the same treatment of evapotranspiration, outflow rates are calculated as more than twice those under Scenario 2 and as in Scenario 3, and percolation rates are greatly underestimated. Essentially, the assumption of evapotranspiration as a single hydrologic pathway similar to evaporation or as two distinct hydrologic pathways (evaporation and transpiration) greatly affects the resulting calculations.

This issue is most important when interpreting flow data from long residence time wetlands. The agricultural and non-agricultural wetlands were operated under inflow HLRs of less than 2 cm d^{-1} during the summer and averaged around 1 cm d^{-1}. During that time, evaporation losses are around 0.8 cm d^{-1}. Under these types of low residence time systems, typical of rice agricultural wetlands (Bachand and Associates et al., 2006) and other non-tidal wetlands (Siegel et al., 2011), transpiration losses to the root zone are a significant sink. Aggregating evaporation and transpiration into a single term risks incorrect interpretation of wetland data and risks incorrect prediction of future outcomes.

4.3. Why transpiration matters — diel and seasonal changes in subsurface fluxes

Despite the importance of transpiration in agricultural literature, (Mmolawa and Or, 2000), much of the work on aquatic crops comes from wetland studies where agronomic principles on constituent transport are not clearly applied (Kadlec, 2000; Bethune et al., 2001; Acreman et al., 2003; Favero et al., 2007). Some of the wetland literature discusses transpiration fluxes with regard to constituent transport (Reddy et al., 1999; Kadlec, 1999) and how those fluxes are greater than diffusive fluxes. We agree with that assessment and have hypothesized that in wetland systems with rooted macrophytes, transpiration results in seasonal and diel patterns in subsurface flow paths. Through our soil flux model, we show diel and seasonal patterns in transpiration (Figs. SI 9, SI 10) result in diel and seasonal changes in transition depth, Z_{trans}, which delineates zones of diffusion dominated fluxes from zones of advection dominated fluxes (Figs. 5, 6). These patterns have important physical and biogeochemical implications. Our model shows that during months for which ET is occurring, only the upper sediment layers are diffusion dominated. For inorganic Hg, the diffusion coefficient has been measured in the range of 5–13 × 10^{-6} cm^2 s^{-1} (0.4–1.1 cm^2 d^{-1}; Holmes and Lean, 2006; Gill et al., 1999) similar to rates measured by others for nitrate (3–30 × 10^{-6} cm^2 s^{-1}; Romkens and Bruce, 1964; Krottje, 1980; Reddy et al., 1980, 1984). In Figs. 5 and 6 we define the low to high diffusion coefficients for inorganic Hg as 5–13 × 10^{-6} cm^2 s^{-1}. For dissolved constituents with similar diffusion coefficient, Z_{trans} is about 0.5–1 cm during the summer in wetland systems. However, some dissolved constituents are stickier. For instance, ammonia diffusion coefficient has been measured by Reddy et al. (1984) in the range of 0.2–9.8 × 10^{-6} cm^2 s^{-1}; an order of magnitude less than inorganic Hg. For these stickier constituents, only the top few millimeters or less are diffusion dominated during periods when ET is occurring. Methylmercury diffusion rates have even been measured as lower (Heirn, 1996). As the diffusion rates become less, Z_{trans} becomes proportionally smaller.

Experimental and comparative field data from Windham-Myers et al. (in this issue-b) support this calculation. Windham-Myers et al. (in this issue-b) found evidence for plants actively moving water and dissolved constituents into the root zone for uptake and for release into the atmosphere during periods of high plant ET (Lindberg et al., 2002, 2005; Reid and Jaffé, 2012). While Hg^0 transport and atmospheric fluxes were not assessed in this study, Windham-Myers et al. (in this issue-b) found 13–37% (median = 22%) greater concentrations of porewater Cl in vegetated soils than in experimentally devegetated plots. Sediment Hg concentrations were similar between experimental treatments, but MeHg concentrations in sediment were elevated (median = 38%) in the presence of vegetation, illustrating the difficulty in teasing apart MeHg production from MeHg concentration in the rhizosphere, both of which are likely occurring. Methylmercury concentrations were higher in rice and wild rice plant roots (median range = 3–12 ng g^{-1}, Windham-Myers et al., in this issue-c) than in surrounding sediments, but is likely a function of both production and

rhizoconcentration. Maximum root depths of 20–24 cm were observed in rice agriculture, and 30 cm in wild rice agriculture, with roots concentrated in the upper 0–5 cm in all fields (Windham-Myers et al., in this issue-c).

Transpiration may also have biogeochemistry implications through the creation of a biogeochemical barrier in the rhizosphere and these biogeochemical barriers may migrate up and down the root zone on a seasonal and diel basis. Reddy et al. (1989) report that microzones around plants affect biogeochemical cycling in the root zones and subsequently constituent transport. In a similar fashion, transpiration may be affecting redox conditions near the soil–water interface as advection transport oxidants past the interface. A migrating oxygen and nitrate front may therefore be enhancing nitrification/denitrification cycling that occurs in wetland systems (Bachand and Horne, 2000a, 2000b; Beauchamp et al., 1989; Weier et al., 1993). In addition, sulfate and iron reduction rates in the root zones may be following diel or seasonal patterns. These resulting changes could affect Hg methylation rates and efficiencies in wetlands (Compeau and Bartha, 1985; Gilmour et al., 1992; Krabbenhoft et al., 1995; Driscoll et al., 1998; Benoit et al., 1999; Mehrotra and Sedlak, 2005) by changing the redox profile and distribution in the root zone, especially near the sediment–water interface through which MeHg must be released before entering the water column. Iron (Fe) speciation, especially the presence of amorphic Fe(III), suggests the presence of plant activity in these wetlands influenced redox sensitive species, at least partially, through transpirative water movement as well as radial oxygen loss (Windham-Myers et al., in this issue-b).

In the case of MeHg, these processes may be contributing to diel and seasonal trends in wetland MeHg cycling. Naftz et al. (2011) reported that the diurnal MeHg concentration in the water column consistently decreased during daylight periods and increased during non-daylight periods in a wetland along the Great Salt Lake. Such patterns are consistent if we consider a system where dissolved constituents are released from the root zone during nocturnal periods when transpiration, and subsequently downward advective flux, decreases. Fleck et al. (USGS, unpublished) found similar diel MeHg trends occurring at these agricultural wetlands. Similarly, Bachand et al. (in this issue) report seasonal changes in MeHg cycling suggesting that plants are moving MeHg into the root zone during summer months when transpiration is occurring and that elevated sediment concentrations lead to a release of MeHg back into the water column in winter when transpiration ceases.

Transpiration thus drives advective transport and based upon our calculations creates a physical barrier against upward migration of dissolved constituents in the soil into the water column. It is another mechanism affecting benthic fluxes. Biological irrigation is defined as a process in which benthic organism activities enhance the exchange of interstitial pore water over pure diffusion (Choe et al., 2004; Hammond et al., 1985). Transpiration is another biological process that could potentially be included in this definition.

4.4. Why transpiration matters — assumptions made during direct diffusion measurements

In situ diffusion coefficient calculations have been estimated employing Fick's First Law and using field determined concentration gradients in the soils (Gill et al., 1999; Holmes and Lean, 2006). However, these estimates assume no disturbance or competing processes occurring during measurement periods. During transpiration, advective flux would be expected to affect concentrations of dissolved constituents in the root zone; thus measuring diffusion coefficients while ET is occurring may lead to confounded data. In support of transpiration's effect on pore water chemistry, Windham-Myers et al. (in this issue-b) noted 13–37% of pore water Cl (used as a conservative tracer) found in the root zone of agricultural wetlands from enhanced transpiration.

5. Conclusion

Through integrating hydrologic and mass budgets using EC as a natural conservative tracer, we quantified evaporation and transpiration rates for agricultural wetlands during the irrigation season. We utilized two reactor models, a PFR and a CFSTR, and through those models bracketed transpiration rates during the irrigation season between 55% (CFSTR)–74% (PFR) of ET rates. This result is consistent with ratios determined in other wetland and shallow aquatic systems through methods of direct measurement (Herbst and Kappen, 1999; Sanchez-Carrillo et al., 2004; Bouman et al., 2005). Of the two reactor models used, the PFR model is more appropriate based upon our statistical analyses of the data for the different agricultural wetlands used and the agricultural wetland configuration. PFR models are expected to approximate non-ideal systems in which ponds are in series, consistent with checks in rice and wild rice systems. We quantified the importance of transpiration with regard to fluxes in the shallow root zone through development of a flux model of diffusive and advective fluxes. Diffusion fluxes used a diffusion coefficient range for inorganic Hg and MeHg from the literature. Our goal was to assess with this model the root zone depths dominated by diffusive fluxes and advective fluxes, as has been done using the Peclet number in groundwater and surface water systems. From our model we defined a transitional depth within the root zone in delineating zones dominated by diffusive fluxes as compared to advective fluxes. Our calculations showed that during active ET, fluxes throughout the root zone are dominated by advective fluxes except in the top millimeters to top centimeter, depending upon the dissolved constituent and its stickiness (mass diffusion coefficient). This transition depth has diel and seasonal trends, tracking ET trends.

These findings challenge the current science foundations. Though fundamental for terrestrial crops in which agronomic principles have been applied, transpiration as a hydrologic transport pathway has generally been ignored for these types of systems. Neglecting this pathway leads to misallocations of load along different hydrologic pathways. Seasonal and diel trends in surface water quality data are potentially confounded by pore water hydrologic trends affected by transpiration. These risks are especially high in wetlands of slow horizontal surface flow, dense vegetation, and thus high water residence times, in which ET is a significant hydrologic sink. Moreover, this process may be affecting the basic assumptions behind methods used for in situ measurements of soil hydrologic and biogeochemical processes. Pore water chemistry through the shallow root zone is likely affected by transpiration through its effect on pore water hydrology and constituent transport, confounding measurements used for calculating diffusion gradients.

We recommend that studies of wetland systems separate E and T from ET in their analyses. We provide an equation for that purpose using flow data and concentration data for natural conservative tracers, such as EC and chloride.

Acknowledgments

The authors wish to thank the significant efforts of reviewers, including James Kuwabara (USGS), Sujoy Roy (TetraTech) and especially the journal associate editor Mae Gustin, for their comments and guidance in greatly improving the utility of the manuscript. Stephanie Fong and Janice Cooke of the Regional Water Quality Control Board and Chris Thompson of San Jose State University Foundation for contract management, David Feliz, Chris Rocco, and Levi Souza of the California Dept. of Fish and Game for logistical support and assistance with sampling, and Jack DeWit of DeWit Farms for cooperation during sampling. This work was funded by the California State Water Resources Control Board under the Proposition 40/50 Agriculture Water Quality Grant Program.

ARTICLE IN PRESS

Appendix A. Supplementary data

Supplementary data to this article can be found online at http://dx.doi.org/10.1016/j.scitotenv.2013.11.026.

References

Acreman MC, Harding RJ, Lloyd CR, McNeil DD. Evaporation characteristics of wetlands: experience from a wet grassland and a reedbed using eddy correlation measurements. Hydrol Earth Syst Sci 2003;7:11–21.

Allen RG, Pereira LS, Raes D, Smith M. Crop evapotranspiration — guidelines for computing crop requirements. Irrigation and drainage paper 56. Rome, Italy: Food and Agriculture Organization of the United Nations; 1998. [Internet], [cited 2010 Sept 30]. Available from: http://www.fao.org/docrep/X0490E/X0490E00.htm].

Alpers CN, Hunerlach MP, May JT, Hothem RL. Mercury contamination from historical gold mining in California. U.S. Geological Survey Fact Sheet 2005–3014; 2005 [Internet], Available from: http://water.usgs.gov/pubs/fs/2005/3014/].

Alpers CN, Fleck JA, Marvin-DiPasquale M, Stricker CA, Stephenson M, Taylor HE. Mercury cycling in agricultural and managed wetlands, Yolo Bypass, California: spatial and seasonal variations in water quality; 2013 [in this issue].

Bachand & Associates, Hydrofocus, Inc., University of California, Davis, U.S. Geological Survey, Ducks Unlimited, Contra Costa Water District. Reducing non-point DOC and nitrogen exports from rice fields: a pilot study and quantitative survey to determine the effects of different hydrologic management practices. Deliverable 15.3 Final Report; 2006. [Auburn (CA): 2006 May. SWRCB Agreement No.: 03-165-555-0].

Bachand PAM, Horne AJ. Denitrification in constructed free-water surface wetlands: I. Very high nitrate removal rates in a macrocosm study. Ecol Eng 2000a;14:9–15.

Bachand PAM, Horne AJ. Denitrification in constructed free-water surface wetlands: II. Vegetation community effects. Ecol Eng 2000b;14:17–32.

Bachand PAM, Bachand S, Fleck J, Alpers CN, Stephenson M, Windham-Myers L. Net methylmercury production and export from agricultural wetlands (rotational rice) in California, USA: revelations from hydrologic analysis; 2013 [in this issue].

Beauchamp EG, Trevors JT, Paul JW. Carbon sources for bacterial denitrification. Adv Soil Sci 1989;10:113–42.

Benoit JM, Gilmour CC, Mason RP, Heyes A. Sulfide controls on mercury speciation and bioavailability to methylating bacteria in sediment pore waters. Environ Sci Technol 1999;33:951–7.

Bethune M, Austin N, Maher S. Quantifying the water budget of irrigated rice in the Shepparton irrigation region, Australia. Irrig Sci 2001;20:99–105.

Bouman BAM, Wopereis MCS, Kropfff MJ, Tenberge HFM, Tuong TP. Water use efficiency of flooded rice agricultural wetlands II. Percolation and seepage losses. Agric Water Manage 1994;26:291–304.

Bouman BAM, Peng S, Castaneda AR, Visperas RM. Yield and water use of irrigated tropical aerobic rice, systems. Agric Water Manage 2005;74:87–105.

Bouman BAM, Humphreys E, Tuong TP, Barker. Rice and water. In: Sparks DL, editor. Adv Agron, 92. ; 2007. p. 187–237.

Bourdreau BP. The diffusive tortuosity of fine-grained unlithified sediments. Geochim Cosmochim Acta 1996;60:3139–42.

Brady NC, Weil RR. The nature and properties of soils. 13th ed. Upper Saddle River: Prentice Hall; 2002.

Burian K. Das Schilfgürtel-Ökosystem eines Steppensees. In: Ellenberg H, editor. Ökosystemforschung. Berlin: Springer; 1973. p. 61–78.

Carleton NJ, Montas HJ. Stochastic modeling of reactive transport in wetlands. Adv Water Resour 2009;32:1615–31.

Carleton JN, Grizzard TJ, Godrej AN, Post HE. Factors affecting the performance of stormwater treatment wetlands. Wat Res 2001;35(6):1552–62.

Choe KY, Gill GA, Lehman RD, Han S, Heim WA, Coale KH. Sediment–water exchange of total mercury and monomethyl mercury in the San Francisco Bay-Delta. Limnol Oceanogr 2004;49:1512–27.

Compeau BC, Bartha R. Sulfate-reducing bacteria: principal methylators of mercury in anoxic estuarine sediment. Appl Environ Microbiol 1985;50:498–502.

Cushman-Roisin B, Beckers JM. Introduction to geophysical fluid dynamics. Physical and numerical aspects, vol. 101. Academic Press; 2011.

Dacey JH, Howes BL. Water uptake by roots controls water table movement and sediment oxidation in short Spartina marsh. Science 1984;224:487–9.

Drexler JZ, Anderson FE, Snyder RL. Evapotranspiration rates and crop coefficients for a restored marsh in the Sacramento–San Joaquin Delta, California, USA. Hydrol Process 2008;22:725–35.

Driscoll CT, Holsapple J, Schofield CL, Munson R. The chemistry and transport of mercury in a small wetland in the Adirondack region of New York, USA. Biogeochemistry 1998;40:137–46.

Dunne EJ, Clark MW, Mitchell J, Jawitz JW, Reddy KR. Soil phosphorus flux from emergent marsh wetlands and surrounding grazed pasture uplands. Ecol Eng 2010;36:1392–400.

Fanjul E, Bazterrica MC, Escapa M, Grela MA, Iribarne O. Impact of crab bioturbation on benthic flux and nitrogen dynamics of Southwest Atlantic intertidal marshes and mudflats. Estuar Coast Shelf Sci 2011;92:629–38.

Favero L, Mattiuzzo E, Franco D. Practical results of a water budget estimation for a constructed wetland. Wetlands 2007;27:230–9.

Freeze RA, Cherry JA. Groundwater. Prentice Hall: Englewood Cliffs, NJ; 1979.

Gill GA, Bloom NS, Cappellino S, Driscoll CT, Dobbs C, McShea L, et al. Sediment–water fluxes of mercury in Lavaca Bay, Texas. Environ Sci Technol 1999;33:663–9.

Gilmour CG, Henry EA, Mitchell R. Sulfate stimulation of mercury methylation in freshwater sediments. Environ Sci Technol 1992;26:2281–7.

Hammond Douglas E, Fuller Christopher, Harmon Dana, Hartman Blayne, Korosec Michael, Miller Laurence G, et al. Benthic fluxes in San Francisco Bay. Temporal dynamics of an estuary: San Francisco Bay. Netherlands: Springer; 1985. p. 69–90.

Hatala JA, Detto M, Sonnentag O, Deverel SJ, Verfaille J, Baldocchi DD. Greenhouse gas (CO2, CH4, H2O) fluxes from drained and flooded agricultural peatlands in the Sacramento–San Joaquin Delta. Agric Ecosyst Environ 2012;150:1–18.

Hayashi TM, Van der Kamp G, Rudolph DL. Water and solute transfer between a prairie wetland and adjacent uplands. 2. Chloride cycle. J Hydrol 1998;207:56–67.

Heald CC, editor. Cameron hydraulic data. Flowserve Corporation; 2002.

Heirn JK. Modelling the fate of mercury in the Carson River and Lahontan Reservoir, Nevada. [Dissertation 3762]Reno, USA: University of Nevada; 1996.

Herbst M, Kappen L. The ratio of transpiration versus evaporation in a reed belt as influenced by weather conditions. Aquat Bot 1999;63:113–25.

Holmes J, Lean D. Factors that influence methylmercury flux rates from wetland sediments. Sci Total Environ 2006;368:306–19.

Howes BL, Dacey JWH, Goehringer DD. Factors controlling the growth form of *Spartian alterniflora*: feedbacks between above-ground production, sediment oxidation, nitrogen and salinity. J Ecol 1986;74:881–98.

Kadlec RH. Detention and mixing in free water wetlands. Ecol Eng 1994;3:345–80.

Kadlec RH. Transport of phosphorus in wetlands. In: Reddy KR, et al, editors. Phosphorus biogeochemistry in subtropical ecosystems. Boca Raton, FL: Lewis Publ.; 1999. p. 355–75.

Kadlec RH. The inadequacy of first-order treatment wetland models. Ecol Eng 2000;15:105–19.

Kadlec RH, Knight RL. Treatment wetlands. Boca Raton: Lewis Publishers; 1996.

Kiendl J. Zum Wasserhaushalt des Phragmitetum communis und des Glycerietum aquaticae. Ber Dtsch Bot Ges 1953;66:246–63.

Krabbenhoft DP, Benoit JM, Babiarz CL, Hurley JP, Andren AW. Mercury cycling in the Allequash Creek watershed, northern Wisconsin. Water Air Soil Pollut 1995;80:425–33.

Krottje PA. Denitrification and nitrous oxide production in Florida wetland soils. [Ms Thesis]Gainesville: University of Florida; 1980.

Kuwabara J, Berelson WM, Balistrieri LS, Woods PF, Topping B, Steding DJ, et al. Benthic flux of metals and nutrients into the water column of Lake Coeur d'Alene, Idaho: report of an August, 1999 pilot study. USGS. Water Resources Investigations Report. 1999. Report No.: 00-4132; 1999.

Kuwabara JS, Topping BR, Carter JL, Wood TM, Cameron JM, Asbill-Case J, et al. Changes in benthic nutrient sources within a wetland after hydrologic reconnection. Environ Toxicol Chem 2012;31:1995–2013.

Langer CS, Fitzgerald WF, Visscher PT, Vandal GM. Biogeochemical cycling of methylmercury at Barn Island Salt Marsh, Stonington, CT, USA. Wetl Ecol Manage 2001;9:295–310.

Lindberg SE, Dong W, Meyers T. Transpiration of gaseous elemental mercury through vegetation in a subtropical wetland in Florida. Atmos Environ 2002;36:5207–19.

Lindberg SE, Donga, Chanton WJ, Qualls RG. A mechanism for bimodal emission of gaseous mercury from aquatic macrophytes. Atmos Environ 2005;39:1289–301.

Liu CW, Chen SK, Jou SW, Kuo SF. Estimation of the infiltration rate of a paddy. Agric Syst 2001;68:41–54.

Martinez CJ, Wise WR. Analysis of constructed treatment wetland hydraulics with the transient storage model OTIS. Ecol Eng 2003;20:211–22.

Marvin-DiPasquale M, Windham-Myers L, Agee JL, Kakouros E, Kieu LH, Fleck J, Alpers CN, Stricker C. Methylmercury production in sediment from agricultural and non-agricultural wetlands in the Yolo Bypass, California; 2013 [in this issue].

Mehrotra AS, Sedlak DL. Decrease in net mercury methylation rates following iron amendment to anoxic wetland sediment slurries. Environ Sci Technol 2005;39:2564–70.

Metcalf L, Eddy HP. Wastewater engineering: treatment, disposal, reuse. New York: McGraw-Hill; 2009.

Mitsch W, Gosselink J. Wetlands. 2nd ed. New York: Van Nostrand Reinhold; 1993.

Mmolawa K, Or D. Root zone solute dynamics under drip irrigation: a review. Plant and Soil 2000;222:163–90.

Naftz DL, Cederberg JR, Krabbenhoft DP, Beisner KR, Whitehead J, Gardberg J. Diurnal trends in methylmercury concentration in a wetland adjacent to Great Salt Lake, Utah, USA. Chem Geol 2011;283:78–86.

Parsons DF, Hayashi M, Van der Kamp G. Infiltration and solute transport under a seasonal wetland: bromide tracer experiments in Saskatoon, Canada. Hydrol Process 2004;18:2011–27.

Pellerin BA, Wollheim WM, Feng X, Vorosmarty CJ. The application of electrical conductivity as a tracer for hydrograph separation in urban catchments. Hydrol Process 2007;22:1810–8.

Penman HL. Natural evaporation from open water, bare soil and grass. Proc R Soc Lond A Math 1948;193:120–46.

Persson J, Wittgren HB. How hydrological and hydraulic conditions affect performance of ponds. Ecol Eng 2003;21(4):259–69.

Playan E, Perez-Coveta O, Martinez-Cob A, Herrero J, Garcie-Navarro P, Latorre B, et al. Overland water and salt flows in a set of rice paddies. Agric Water Manage 2008;95:645–58.

Raven PH, Evert RF, Eichhorn SE. Biology of plants. New York, NY: W.H. Freeman and Company; 1999 [944 pp.].

Reddy KR, Patrick Jr WH, Phillips RE. Evaluation of selected processes controlling nitrogen loss in a flooded soil. Soil Sci Soc Am J 1980;44:1241–6.

Reddy KR, Patrick WH, Broadbent FE. Nitrogen transformations and loss in flooded soils and sediments. Crit Rev Environ Sci Technol 1984;4:273–309.

Reddy KR, Patrick Jr WH, Lindau CW. Nitrification–denitrification at the plant root–sediment interface in wetlands. Limnol Oceanogr 1989;34(6):1004–13.

Reddy KR, Kadlec RH, Flaig E, Gale PM. Phosphorus retention in streams and wetlands: a review. Crit Rev Environ Sci Technol 1999;29(1):83–146.

Please cite this article as: Bachand PAM, et al, Differentiating transpiration from evaporation in seasonal agricultural wetlands and the link to advective fluxes in the root zone, Sci Total Environ (2013), http://dx.doi.org/10.1016/j.scitotenv.2013.11.026

ARTICLE IN PRESS

Reid MC, Jaffé PR. Gas-phase and transpiration-driven mechanisms for volatilization through wetland macrophytes. Environ Sci Technol 2012;46(10):5344–52.

Romkens JJM, Bruce RR. Nitrate diffusivity in relation to moisture content of non-adsorbing porous media. Soil Sci 1964;98:332–7.

Rosenberry DO, Sheibley RW, Cox SE, Simonds FW, Naftz DL. Temporal variability of exchange between groundwater and surface water based on high-frequency direct measurements of seepage at the sediment–water interface. Water Resour Res 2013;49:2975–86.

Rothenberg SE, Ambrose RF, Jay JA. Mercury cycling in surface water, pore water and sediments of Mugu Lagoon, CA, USA. Environ Pollut 2008;154:32–45.

Sanchez-Carrillo SDG, Angeler DG, Sanchez-Andres R, Alvarez-Cobelas M, Garatuza-Payan J. Evapotranspiration in semi-arid wetlands: relationships between inundation and the macrophyte-cover: open-water ratio. Adv Water Resour 2004;27:643–55.

Shuttleworth WJ, Wallace JS. Evaporation from sparse crops — an energy combination theory. Q J R Meteorol Soc 1985;111:839–55.

Siegel S, Bachand P, Gillenwater D, Chappell S, Wickland B, Rocha O, et al. Final evaluation memorandum, strategies for resolving low dissolved oxygen and methylmercury events in northern Suisun Marsh. Report prepared for the State Water Resources Control Board; 2011 [Sacramento (CA): 2011 May. SWRCB Project No.: 06-283-552 0. May].

Soilweb. Streaming, seamless interface to USDA-NCSs SSURGO and STATSGO Soil Survey Products. Soil Resource Lab, University of California Davis; 2011 [Copyright 2008. Accessed September 15, 2011].

Springborn M, Singer MB, Dunne T. Sediment-adsorbed total mercury flux through Yolo Bypass, the primary floodway and wetland in the Sacramento Valley, California. Sci Total Environ 2011;412:203–13.

Taiz L, Zeiger E. Plant physiology. Redwood City: The Benjamin/Cummins Publishing Co.; 1991 [565 pp.].

Tchobanoglous G, Schroeder ED. Water quality: characteristics, modeling, modification. Reading: Addison-Wesley; 1985.

Van der Kamp G, Hayashi M. Groundwater–wetland ecosystem interaction in the semiarid glaciated plains of North America. Hydrogeol J 2009;17:203–14.

Weier KL, Doran JW, Power JF, Walters DT. Denitrification and the dinitrogen:nitrous oxide ratio as affected by soil water, available carbon, and nitrate. Soil Sci Soc Am J 1993;57:66–72.

Werner TM, Kadlec RH. Wetland residence time distribution modeling. Adv Water Resour 2001;32:1615–31.

Whitmer S, Baker L, Wass R. Loss of bromide in a wetland tracer experiment. J Environ Qual 2000;29:2043–5.

Windham-Myers L, Ackerman JT, Fleck JA, Marvin-DiPasquale M, Stricker CA, Bachand P, et al. Mercury cycling in agricultural and managed wetlands: a synthesis of observations from an integrated field study of methylmercury production, hydrologic export, and bioaccumulation; 2013a [in this issue, a].

Windham-Myers L, Marvin-DiPasquale M, Stricker C, Agee JL, Kieu L, Kakouros E. Mercury cycling in agricultural and managed wetlands, Yolo Bypass, California: experimental evidence of vegetation-driven changes in sediment biogeochemistry and methylmercury production; 2013b. http://dx.doi.org/10.1016/j.scitotenv.2013.05.028 [in this issue, b].

Windham-Myers L, Marvin-DiPasquale M, Kakouros E, Agee JL, Kieu LH, Stricker C, et al. Mercury cycling in agricultural and managed wetlands, Yolo Bypass, California: seasonal influences of vegetation on mercury methylation, storage, and transport; 2013c. http://dx.doi.org/10.1016/j.scitotenv.2013.05.028 [in this issue, c].

Wopereis MPS, Bouman BAM, Kropff MJ, Tenberge HFM, Maligaya AR. Water use efficiency of flooded rice agricultural wetlands I. Validation of the soil-hydrologic balance model SAWAH. Agric Water Manage 1994;26:277–89.

Please cite this article as: Bachand PAM, et al, Differentiating transpiration from evaporation in seasonal agricultural wetlands and the link to advective fluxes in the root zone, Sci Total Environ (2013), http://dx.doi.org/10.1016/j.scitotenv.2013.11.026